AD A038085

REPORT NVL-0059-003

(4) NVL

STUDY OF ELECTRONIC TRANSPORT AND BREAKDOWN IN THIN INSULATING FILMS

Walter C. Johnson
PRINCETON UNIVERSITY
Department of Electrical Engineering
Princeton, New Jersey 08540
Telephone: (609) 452-4621

1 December 1976

SEMI-ANNUAL TECHNICAL REPORT NO. 2

Approved for public release; distribution unlimited.

DDC
MAR 31 1977
C

Prepared for:

NIGHT VISION LABORATORY
U. S. Army Electronics Command
Fort Belvoir, Virginia 22060

Sponsored by:

DEFENSE ADVANCED RESEARCH PROJECTS AGENCY

DARPA Order No. 2182
Program Code. No. 6D10
Contract DAAG53-76-C-0059
Effective Date: 17 November 1975
Expiration Date: 31 December 1977

DDC FILE COPY

The views and conclusions contained in this document are those of the authors and should not be interpreted as necessarily representing the official policies, either expressed or implied, of the Defense Advanced Research Projects Agency of the U. S. Government.

Unclassified

SECURITY CLASSIFICATION OF THIS PAGE (When Data Entered)

REPORT DOCUMENTATION PAGE

READ INSTRUCTIONS BEFORE COMPLETING FORM

1. REPORT NUMBER: NVL-0059-003	2. GOVT ACCESSION NO.
3. RECIPIENT'S CATALOG NUMBER	
4. TITLE (and Subtitle): STUDY OF ELECTRONIC TRANSPORT AND BREAKDOWN IN THIN INSULATING FILMS.	5. TYPE OF REPORT & PERIOD COVERED
	6. PERFORMING ORG. REPORT NUMBER
7. AUTHOR(s): Walter C. Johnson Telephone: (609) 452-4621	8. CONTRACT OR GRANT NUMBER(s): DAAG53-76-C-0059, DARPA Order-2182
9. PERFORMING ORGANIZATION NAME AND ADDRESS: Princeton University Department of Electrical Engineering Princeton, New Jersey 08540	10. PROGRAM ELEMENT, PROJECT, TASK AREA & WORK UNIT NUMBERS: 61101E, ARPA 2182, 6D10, 024Cj
11. CONTROLLING OFFICE NAME AND ADDRESS: Defense Advanced Research Projects Agency 1400 Wilson Boulevard Arlington, Virginia 22209	12. REPORT DATE: 1 Dec [redacted]76 13. NUMBER OF PAGES: 69
14. MONITORING AGENCY NAME & ADDRESS (if different from Controlling Office): Night Vision Laboratory DRSEL-NV-II Fort Belvoir, Virginia 22060	15. SECURITY CLASS. (of this report): Unclassified 15a. DECLASSIFICATION/DOWNGRADING SCHEDULE

16. DISTRIBUTION STATEMENT (of this Report)

Approved for public release; distribution unlimited.

Semi-annual technical rpt. no. 2,

17. DISTRIBUTION STATEMENT (of the abstract entered in Block 20, if different from Report)

18. SUPPLEMENTARY NOTES

The work reported herein is a continuation of research initiated under ARPA Order No. 2180, monitored by Air Force Cambridge Research Laboratories (LQ).

19. KEY WORDS (Continue on reverse side if necessary and identify by block number)

Insulating Films
Electronic Transport in Insulators
Charge Trapping in Insulators
Dielectric Breakdown
Silicon Dioxide

20. ABSTRACT (Continue on reverse side if necessary and identify by block number)

Recent progress is reported on an ongoing program of studies of high-field electronic injection, transport, trapping, and dielectric breakdown in thin insulating films. The studies include the use of combined corona and optical techniques for the investigation of carrier injection, transport, and trapping; a study of the charge-carrier recombination properties of SiO_2 and the Si-SiO_2 interface; an investigation of the high-field generation of electron traps in MOS structures; a study of high-field breakdown effects in aluminum oxide; and an investigation of electron-beam-induced interface states in the Si-SiO_2 system.

DD FORM 1 JAN 73 1473 EDITION OF 1 NOV 65 IS OBSOLETE S/N 0102-014-6601

Unclassified 400 734

SECURITY CLASSIFICATION OF THIS PAGE (When Data Entered)

TABLE OF CONTENTS

Page

1. Introduction 1

2. Further Studies of Thin Insulating Films by the Combined Corona-Photoemission Method (H.H. Chao collaborating)

   2.1. Introduction 3

   2.2. Light-Induced Surface Discharge After Negative Surface Charging of SiO_2 4

   2.3. Study of Electron Traps Generated by Negative Corona 13

3. Recombination in Thermally Grown Silicon Dioxide (J.J. Clement collaborating)

   3.1. Introduction 19

   3.2. Experiments 19

   3.3. Theory 21

   3.4. Results 23

   3.5. Discussion 29

   3.6. Summary 32

4. High-Field Creation of Electron Traps in Silicon Dioxide (C. Jenq collaborating)

   4.1. Introduction 33

   4.2. Experiments 33

   4.3. Results 33

   4.1. Conclusions 41

5. High-Field Charging and Breakdown of Al_2O_3 ..... 42 (O. Bar-Gadda collaborating)

6. High-Field Studies of Aluminum Oxide Films (S. S. Li collaborating)

   6.1. Introduction 48

   6.2. Experimental Results 48

   6.3. Discussion 53

Page

7. Interface State Generation in the Scanning Electron Microscope (P. Roitman collaborating)

7.1. Introduction 54

7.2. Experimental 55

7.3. Results 56

7.4. Discussion 56

REFERENCES

A. Publications, Reports and Doctoral Dissertations Resulting From Work Done Under This Program 63

B. Other References 65



1. INTRODUCTION

We report here on recent progress in an ongoing program of research directed toward a basic understanding of the electronic properties of thin insulating films and of the interfaces of such films with semiconductors and metals. Of particular interest are the high-field properties, including charge-carrier injection through the interfaces, electronic transport through the insulator, charge-carrier trapping and recombination at the interfaces and in the insulator, and the mechanisms leading to dielectric breakdown. The objective of the program is to provide a rational basis for the choice of materials, processing methods and treatment of the insulating films in order to obtain the desired performance and reliability. The insulating films under study at the present time are silicon dioxide, aluminum oxide, and silicon nitride on silicon substrates. The techniques and apparatus that we have developed under this program are, moreover, immediately applicable to the study of other types of insulating films and substrates.

We have previously reported on many of the results of the studies made under this program,[1-26] and additional reports and papers are in preparation. The organization of this report is as follows:

Section 2 describes recent results obtained by use of the combined corona and photoemission technique first described in the preceding Semi-Annual Report.[25] This unusually versatile technique has been developed by H. H. Chao of our staff, and combines the advantages of corona charging to produce the electric field in the insulator,[20] internal photoemission[27] for the independent injection of charge carriers into the insulator, and optical interference techniques for the separation of effects at the front surface from those occurring at the interface with the substrate.[25] Here we discuss new results obtained by use of this method on silicon dioxide. The technique is currently being used in a study of silicon nitride on silicon, and the results of this study will be reported at a later time.

Section 3 describes a recent investigation by J. J. Clement of a property of silicon dioxide that is important to the radiation hardening of MOS devices, namely the charge-carrier recombination properties of the oxide and of the interfacial $Si-SiO_2$ region. His method is based on the observation that at liquid nitrogen temperature, holes are transported

extremely slowly in SiO_2 at weak or moderate fields, whereas electrons have a good mobility. He creates hole-electron pairs in SiO_2 at reduced temperature by irradiation with soft X rays, drifts the electrons out leaving the holes behind, and then injects electrons into the oxide in a controlled manner by internal photoelectric emission. In this way the recombination properties of the holes with the electrons can be examined in a systematic manner. By use of this technique, he has succeeded in measuring the capture cross sections for recombination both in the bulk and at the Si-SiO_2 interface, and has determined the electric-field dependence of these cross sections.

We have previously reported on the generation of interface states in the Si-SiO_2 system under high-field conditions.[25] In pursuing this matter further, C. Jenq has observed a generation of electron traps in the oxide. His observations and conclusions in this regard are given in Section 4.

We have previously noted[17] that a dielectric breakdown event in thermally grown silicon dioxide is preceded by a rise in current through the oxide, and we have interpreted this in terms of a positive-feedback chain of events initiated by Fowler-Nordheim tunneling of electrons from the negative electrode followed by impact ionization in the oxide, and the trapping of impact-produced holes near the negative electrode which results in an increase in the electric field at this interface and an enhancement of the electron tunneling. In light of this, a startling observation has been made recently at Bell Laboratories concerning the breakdown of MOS structures in which the insulator is aluminum oxide: the danger signal for imminent breakdown in aluminum oxide is a decrease, rather than the expected increase, in the current through the oxide. This indicates a different chain of events in aluminum oxide than in silicon dioxide, and is clearly a matter that deserves further investigation. O. Bar-Gadda and S.S. Li of our staff are currently using corona[20] and self-quenching[17] techniques in a study of high-field charge injection and trapping in aluminum oxide as a first step in unraveling the chain of events that results in electrical breakdown of this material. Their preliminary reports on their findings are given in Sections 5 and 6.

P. Roitman is completing a study of lateral nonuniformities in MIS structures using scanning-electron-microscope (SEM) techniques.[13] One of the results of the electron irradiation of an MIS structure is the generation of new electronic states at the insulator-semiconductor interface and a resulting alteration in the characteristics of the MIS device. This effect is of importance not only in SEM work but also in electron-beam lithography. In Section 7 of this report Mr. Roitman gives the results of his study of the electron-beam-induced formation of interface states.

2. FURTHER STUDIES OF THIN INSULATING FILMS BY THE COMBINED CORONA-PHOTOEMISSION TECHNIQUE

(H. H. Chao collaborating)

2.1. Introduction

A background discussion of the combined corona-photoemission technique was given in Sec. 3.1 of Semi-Annual Report No. 1.[25] Briefly stated, a corona discharge is produced in a gas of controlled composition at approximately atmospheric pressure by applying a large d-c voltage (5-10 kV) to a gold needle which is located a short distance ($\sim$ 2-5 cm) from the plane of the sample.[20] The discharge contains both positive and negative ions of species typical of the gas being used. If the needle is positive in polarity, positive ions are repelled to the sample where they charge the unmetallized surface of the insulating film positively. Conversely, if the needle is negative in polarity, negative ions charge the insulator surface negatively. The surface charge produces the electric field required for transport of charge carriers in the insulator. The advantages of this method include the avoidance of destructive breakdown because of the absence of lateral conduction on the surface of the sample[20] and the elimination of the need for a metallic field plate which, in photoelectric studies, would absorb a large portion of the incident light and might also serve as an efficient, but possibly unwanted, source of photoinjected carriers in the insulator.[25]

The original corona method[20,27] relied on the high-field injection of carriers into the insulator; thus the rate of injection and the magnitude

of the transporting field were inextricably linked together. An additional dimension of freedom is added to the experiment by separating the functions of transport and injection. We do this by utilizing internal photoinjection to supply the carriers and relying on the ion-produced electric field only to produce the transporting forces. The use of light to provide the carriers also introduces the possibility of utilizing optical interference in the insulating film to maximize the light intensity at either of the two interfaces and thus provide a means for separating injection effects occurring at the insulator-semiconductor interface from those that may take place at the outer surface. The optical interference technique was discussed in Sec. 3.2 of Semi-Annual Report No. 1.[25]

We have found the study of light-induced surface discharge after positive or negative corona charging to be a particularly effective method for studying injection and transport in the insulator. Section 3.3 of Semi-Annual Report No. 1 described results obtained by positive surface charging of the Si-SiO_2 system.[25] In Sec. 2.2 of the present report we discuss information obtained on this system by negative surface charging, and in Sec. 2.3 we present the results of a study of the electron traps which are found to be generated by negative corona charging.

2.2. Light-Induced Surface Discharge After Negative Surface Charging of the Thermally Grown SiO_2-Si Structure and a CVD SiO_2-Thermally Grown SiO_2-Si Structure

Negative corona in dry air was used to charge the surface to the desired potential. The maximum potentials used in this study correspond to oxide fields of 6×10^6 V/cm. After the corona was shut off, the chamber was pumped down to 10^{-3} torr. If the sample was kept in the dark, no change in surface potential was found after 24 hrs. The output of a Bausch and Lomb monochrometer was used to discharge the surface potential to $V_s = V_{s(initial)} - 2$ volts (unless specified otherwise). After this the chamber was refilled with dry air and negative corona was used to charge the sample to its initial potential. The same process was repeated over a range of photon energies.

The experimental results indicate that the discharge rate depends on the history of the sample. Figure 2.1 shows typical results obtained on a sample designated as P4, which had a 1900 Å film of dry-grown SiO_2 on a 10 Ω-cm p-type (100) silicon substrate. The sample was charged to -58 volts with negative corona and discharged to -55 volts with 5.3 eV light repeatedly. The discharge rate ($\Delta V_s/F$) increased at the beginning, then reached a "steady state". The discharge rate remained in "steady state" when the photon energy was changed. After the foregoing procedure, the sample was charged to -116 volts with negative corona and discharged to -113 volts with 5.3 eV light repeatedly. The discharge rate increased in the first few steps, then reached a "steady state" again. The sample was discharged to -58 volts and the process of charging and discharging was repeated. The discharge rate decreased for the first few steps, then reached the "steady state". Figure 2.2 shows the results obtained on a sample designated as DP7, which had a 4149 Å film of HCl-steam grown SiO_2 on a 0.001 Ω-cm p-type (111) silicon substrate. The general features are the same for the P4 sample except that the discharge rate decreases at the beginning.

We shall now describe the experiments which show that electron injection from the front surface, not hole injection from the silicon substrate, is the dominant process in the light-induced surface discharge of the Si-SiO_2 system after negative charging of the surface. The discharge rate is found to depend on the surface condition which, in turn, depends on the history of the sample.

The experimental data discussed in the following were obtained in the "steady state."

After the discharge experiments, the CV curve of the sample shows no significant stretch-out or flatband-voltage shift. Hence there was no significant charge trapping in these samples.

Figure 2.3 shows $\left[C_i|\Delta V_s|/qRF\right]^{1/3}$ vs. photon energy for two samples: Sample P2, which had 2450 Å of HCl-steam oxide on a 1 ohm-cm (100) p-Si substrate, and Sample P2-E, which is the same as P2 except with 75 Å of the oxide etched off. Utilizing the reasoning of the optical interference method (Sec. 3.2 of Ref. 25), the fact that the structure of T/R does

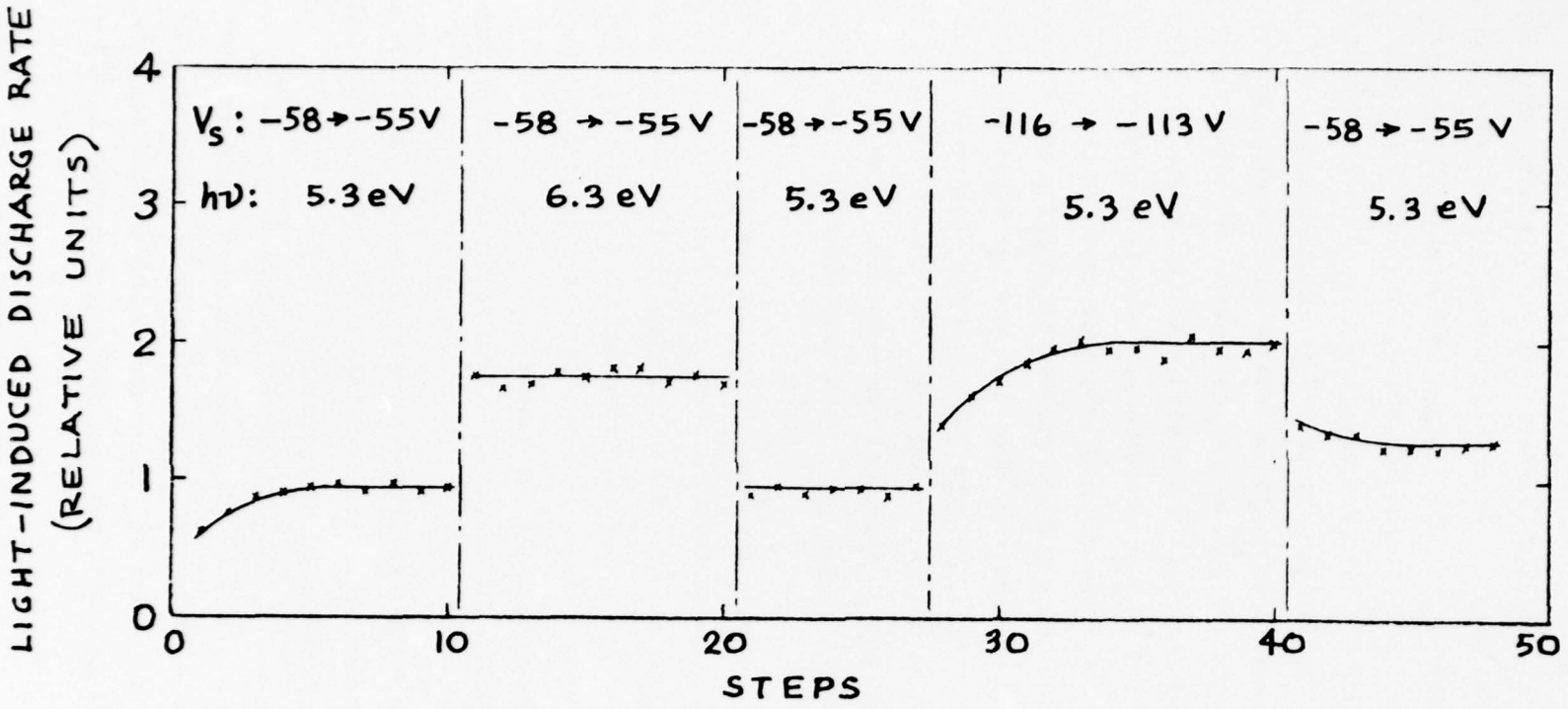


Fig. 2.1. Light-induced discharge rate ($\Delta V_s/F$) versus steps for P4 sample. The sample was charged by negative corona and discharged by UV light repeatedly.

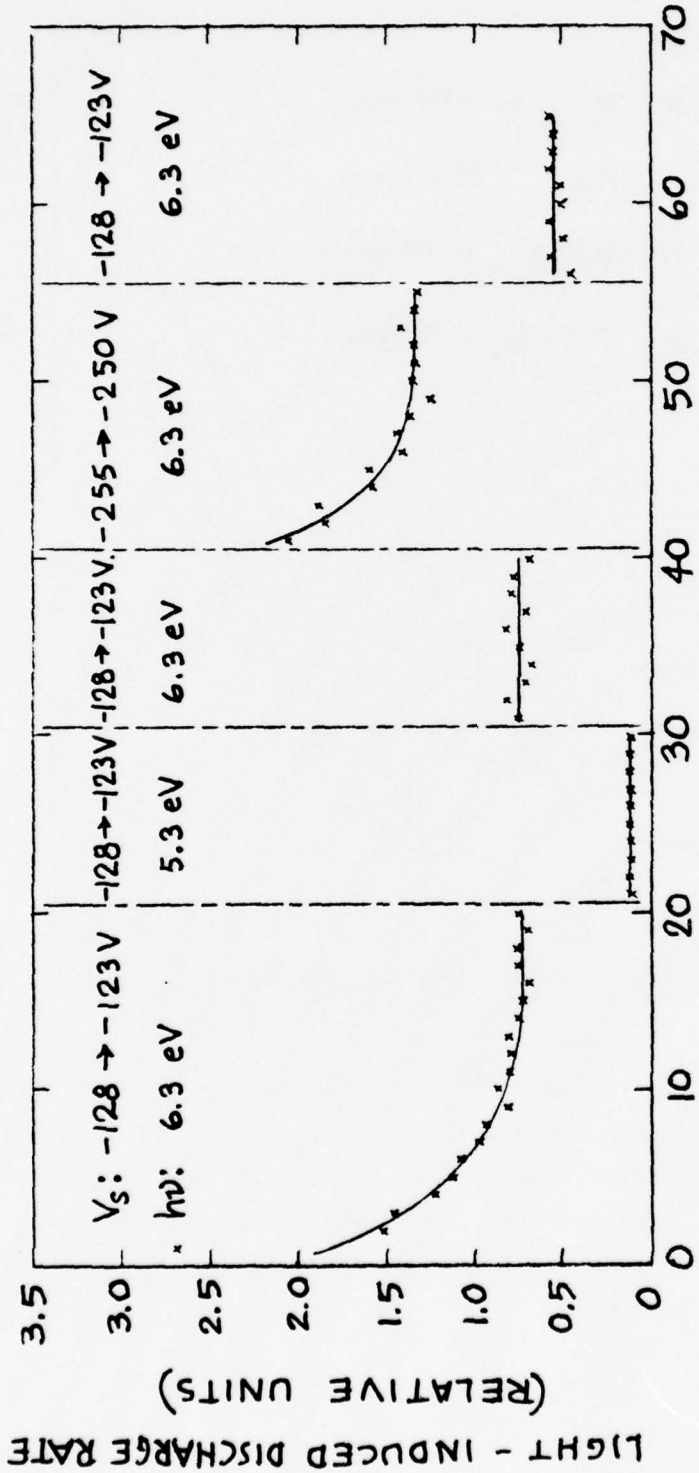


Fig. 2.2. Light-induced discharge rate ($\Delta V_s/F$) versus steps for DP7 sample. The sample was charged by negative corona and discharged by UV light repeatedly.

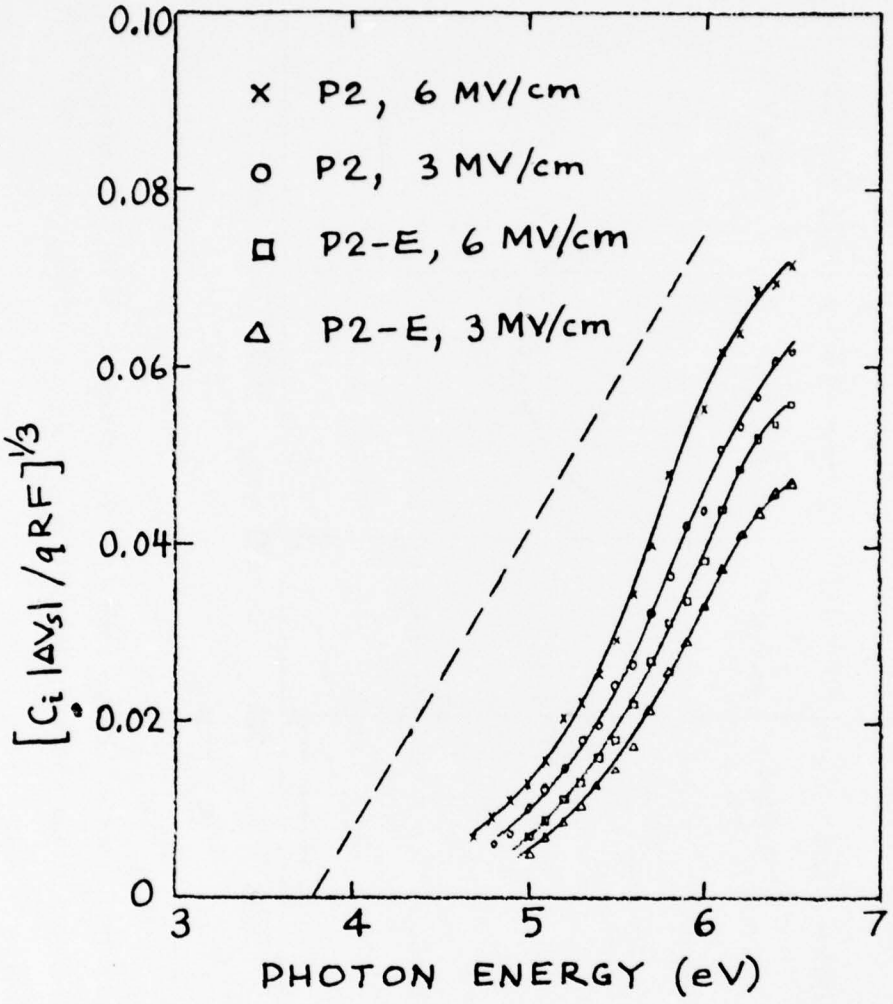


Fig. 2.3. $\left[C_i|\Delta V_s|/qRF\right]^{1/3}$ vs. photon energy for various fields and samples. $C_i|\Delta V_s|/qRF$ is equal to the quantum yield for electron injection from the front surface. The dashed line is the Au-SiO_2 quantum yield for an applied field of 3MV/cm reported by Powell.[29]

not appear in the curves suggests that hole emission from the substrate can be neglected. Hence the quantum yield for electron injection from the front surface charge is[25]

$$\text{Quantum Yield} = C_i |\Delta V_s| / qRF \qquad (2.1)$$

There is additional evidence which shows that electron injection from front surface is the dominant process: the difference between the P2 and P2-E samples indicates that the light-induced discharge rate depends on the surface condition of the sample. The quantum yield of electron injection from the front surface is smaller than that from a metal gate at the same field, as reported by Powell.[29]

The same experiments were conducted on samples which had substrates with different orientations and doping levels and oxides with different growth methods. The results are similar to those results obtained on the P2 and P2-E samples.

It is of interest to consider the approximate upper bound of the hole injection quantum yield. Using the interference technique, the detection of small undulations from the $C_i |\Delta V_s| / qRF^{1/3}$ vs. photon energy plot is difficult because the quantum yield varies over three orders of magnitude for photon energies between 4 and 6.5 eV. However, we should be able to detect modulation amounting to 50% of the average value of the quantum yield. Since $(T/R)_{max.}$ is above five, we conclude that the quantum yield for hole photoemission must be smaller than 10% of the surface electron injection quantum yield. The quantum yield of electron injection from the surface is about one order smaller than the quantum yield of electron injection from a 100 Å gold gate (as reported by Powell[29]), which is one order smaller than the quantum yield of electron injection from Si into SiO_2. Hence the quantum yield of hole injection from Si into SiO_2 should be three orders smaller than the quantum yield of electron injection from Si into SiO_2 for oxide fields of $\sim$ 3 mv/cm.

After the discharge experiment, no significant negative flatband voltage shift was found. This agrees with the result of Woods and Williams;[30]

they were unable to photoinject holes from the silcon and trap them "permanently" in the SiO_2 when they photo-discharged the negatively charged surface, using 7.8 eV photons for this purpose. They explain this result as follows: Almost all of the injected holes were trapped in the SiO_2 within 20 Å of the interface because of the high density of hole traps there. Almost immediately these holes tunnel back into the silicon. Those few holes that escape the traps near the interface are trapped deeper in the oxide. Probably they are then neutralized by electrons which had been photodischarged from the outer surface. The vacuum ultraviolet experiments of Powell and Derbenwick[31] and of Powell and Hughes[32] indicate that only about 50% of the holes are trapped in permanent sites. In reality, probably all of the holes are trapped, but some of them penetrate almost to the silicon surface so that after being trapped, they can tunnel almost immediately into the silicon valence band.

The low injection efficiency of holes from Si into SiO_2[30-35] and the positive charge buildup in the oxide after exposure to ionizing radiation[36] can be explained by this model. The low injection efficiency is due to the high density of hole traps near the interface. The positive charge buildup is due to the hole traps deeper in the oxide (20 Å - 320 Å from the interface.)[30]

According to Woods and Williams' model,[30] the hole trapping should be observed if we can eliminate or reduce the number of electrons coming from the photo-discharging front surface. In order to reduce the electron injection from the front surface, we used UV light with photoenergies corresponding to the minima of R/T.

After charging the surface potential of the P2 sample to -135V (E_{ox} = 5.51 mv/cm) and waiting for 24 hrs, no significant flatband voltage shift could be observed. After this the sample was discharged to -105 V (E_{ox} = 4.29 mv/cm) with 6.2 eV light. The sample was then charged to -130 V and discharged to -105 V again. A flatband voltage shift of -0.5 V was observed* indicating that there were trapped holes in the oxide.

* If we start the C-V trace from a negative value, then as the voltage of the mercury probe is swept in the positive direction, some of the trapped holes are recombined with electrons tunneling from the Si. This effect was avoided by biasing the sample as 5V for 2 min. before taking the C-V curve.

Then the sample was charged to 5 V and discharged to 1 V by 5 eV light. The flatband voltage returned to its initial value (0.25 V) indicating that the trapped holes had been recombined with electrons that were injected from the silicon substrate.

Because R/T (Sec. 3.2, Ref. 25) is maximum for 5.6 eV UV light, there are more electrons available to recombine with the holes. When UV light with photoenergy of 5.6 eV instead of 6.2 eV was used for discharging, no significant flatband voltage shift could be found.

The sample was then charged to -65 V (E_{ox} = 2.65 mv/cm) and discharged to -50 V (E_{ox} = 2.04 mv/cm) by 6.2 eV UV light. This process was repeated twice. No significant flatband voltage shift could be observed. This may be due to the larger capture cross section of electrons by trapped holes at lower fields.[37] Another possible reason is that the location of the potential barrier maximum is much deeper in the oxide at lower fields.

The same experiments were conducted on the P4 sample, with essentially the same results.

This experiment was also conducted on samples on which a layer of CVD SiO_2 (150 Å) had been deposited on top of the thermally grown SiO_2 when UV light was used to discharge the surface after negative surface charging. Almost all of the electrons injected from the front surface were trapped at the interface between the two oxide layers because of the high density of electron traps there. The trapped electrons at the interface between the two oxide layers may be photodepopulated and drifted toward the substrate. That is, we can not prevent the electrons from reaching the Si-SiO_2 interface entirely, but we can reduce the probability substantially.

The sample was charged to -145 V and was discharged to -120 V with 6 eV light twice. A flatband voltage of +2.8 V was observed, thus indicating that there is negative charge storage in the SiO_2. This negative charge is that of the trapped electrons at the interface between the two oxide layers. Then the top 250 Å SiO_2 was etched off with P-etch. The samples were rinsed in distilled water and blown dry with N2. This etch-off process removes the trapped electrons in the oxide. The flatband

voltage was then found to be -2.3 V. This flatband voltage indicates the presence of trapped holes in the oxide. The trapped holes can be annealed by electron injection from Si into SiO_2.

In order to make sure that the observed holes were introduced by the UV light, a sample was charged to -150 V by negative corona and discharged to -90 V by positive corona twice. Then the top 400 Å SiO_2 layer was etched off. The resulting flatband voltage showed no sign of hole trapping.

The trapped holes in the oxide may have been introduced by either of two processes: (1) Holes may have been photoinjected from the Si into the SiO_2 and trapped by the hole traps in the oxide. (2) Electrons may have been photoexcited from neutral centers in the oxide into the oxide conduction band, leaving holes trapped in the centers. Based on an experimental result which will be discussed at the end of the next section, we believe the correct explanation to be the photoinjection of holes from the substrate into the oxide with subsequent trapping in the oxide.

The VUV experiments of Powell[38] show that the probability of a hole being trapped in the SiO_2 as it passes through is a strong function of the processing parameters. This property is an important factor in radiation hardness. However, our experiments show that even for samples that show good radiation hardness, the hole current can be neglected during the light-induced discharge process after negative surface charging. Furthermore, no trapped holes can be found after the discharging process has been completed. We conclude that the density of hole traps near the interface must be very high to prevent holes from being injected from the substrate. Moreover, the density of hole traps deeper in the oxide appears to be low, for holes can be transported through the bulk of the oxide. When such holes reach the traps near the interface they are trapped very close to the interface and can tunnel almost immediately into the valence band of the silicon substrate. This provides an explanation for both the radiation hardness of these oxides and the difficulty observed in injecting holes from the substrate.

2.3. Study of the Electron Traps Generated by Negative Corona

When a thermally grown SiO_2 film is exposed to negative corona at fields greater than about 10 MV/cm, electron trapping centers in the oxide are generated.[22,25] The trapped electrons can be removed by annealing at 150 °C for 30 min in vacuum, and the electron traps themselves can be annealed out at 150°C for 30 min in the presence of an electric field of about 5 MV/cm.[25]

We have conducted additional experiments to reveal the properties of these electron traps. The samples had 1900 Å of dry SiO_2 on 10 ohm-cm (100) p-silicon. Negative corona with a current density of 6×10^{-8} A/cm^2, applied for 15 min, was used to produce the electron traps. This treatment also produces holes which are trapped in the oxide, principally near the interface, and this positive trapped charge obscures the presence of the electron traps. The positive charge can be removed and the electron traps themselves filled with electrons by an injection of electrons into the oxide.[25] For this purpose we utilized an internal photoinjection of electrons from the silicon substrate. The neutralization of the positive charge and the filling of the electron traps was monitored by taking the high-frequency (1 MHz) C-V curve at intervals, using a mercury probe for temporary metallization, and observing the flatband voltage of the structure. After the (positive) flatband voltage shift had saturated, indicating that the positive charge had been neutralized and all of the electron traps filled, the samples were kept in the dark at room temperature for 24 hrs. This resulted in about 10% reduction in flatband voltage, indicating that most of the electron traps were too deep to have appreciable thermal emission at room temperature.

An etch-off experiment was then conducted to determine the spatial distribution of the deeply trapped electrons. The analysis appropriate to this experiment is as follows:

The general expression for the flatband voltage of an MIS structure is

$$V_{fb} = \phi_{MS} - Q_{ss}\, x_o/\epsilon_{ox} - (1/\epsilon_{ox}) \int_o^{x_o} x\rho(x)\, dx \qquad (2.2)$$

where ϕ_{MS} is the metal-semiconductor work function difference, x_o is the

oxide thickness, Q_{ss} is the fixed charge present at the Si-SiO_2 interface, and $\rho(x)$ is the charge distributed through the oxide. The origin of x is at the metal-SiO_2 interface. The coordinate of the Si-SiO_2 interface is x_o.

We assume that Q_{ss} does not change during the experiment. Then

$$V_{FBo} = \phi_{MS} - Q_{ss}x_{oo}/\epsilon_{ox} \tag{2.3}$$

where V_{FBo} is the flatband voltage of the fresh sample (before charging), and x_{oo} is the original thickness of the oxide. From Eqs. (2.2) and (2.3) we have

$$V_{FB}(x_o) - \phi_{MS}(1 - x_o/x_{oo}) + V_{FBo}(x_o/x_{oo}) = \frac{q}{\epsilon_{ox}} \int_o^{x_o} x\, N_t(x)dx \tag{2.4}$$

where q is the magnitude of the electronic charge and $N_t(x)$ is the density of the trapped electrons.

The experiment proceeds as follows. The metal-semiconductor work-function difference, ϕ_{MS}, is presumed to be known, and the flatband voltage of the fresh sample, V_{FBo}, can be measured. The thickness of the oxide, x_o, is the independent variable in the experiment and is reduced in successive steps from its initial value, x_{oo}, by etching the surface. The flatband voltage, $V_{FB}(x_o)$, is the dependent variable and is measured after each etching step. The left side of Eq. (2.4) is then plotted against x_o and yields information concerning $N_t(x)$ as shown by Eq. (2.4).

The results of such an experiment, performed on four similar samples of 1900 Å dry-grown SiO_2, are shown in Fig. 2.4. Each of the solid and dashed curves represents an exponential trapped electron density of the form

$$N_t(x) = B \exp(-x/D) \tag{2.5}$$

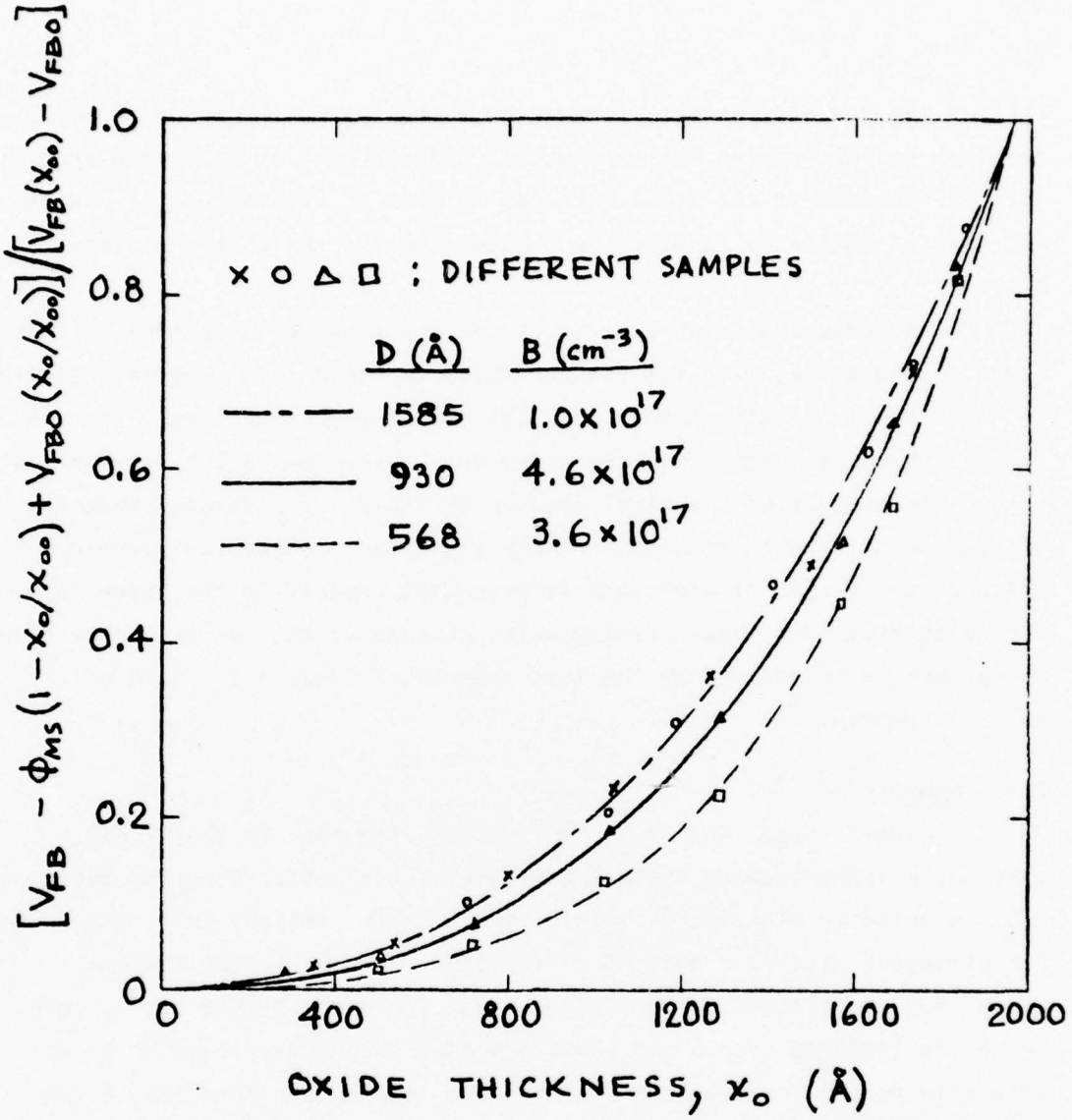


Fig. 2.4. Flatband voltage shift versus thickness of remaining oxide in etch-off experiment to determine the trapped electron distribution. The lines are calculated for a trapped electron density $N_t(x) = B \exp(-x/D)$, where B and D are adjustable parameters.

where B and D are adjustable parameters whose values are shown in the figure. For each of the samples the exponential distribution of trapped electrons, with the maximum at the front surface, is seen to fit very well. We are not able at this time to offer an explanation for the observed distribution.

A photodepopulation experiment was performed to determine the energy level of the traps, with the results shown in Table 4.1. The optical depth of the traps is greater than 4 eV. This is considerably larger than the thermal depth as judged from the previously quoted annealing experiments.

The results of the final process in Table 4.1 indicate that no trapped holes were introduced. If trapped holes had been introduced by the photoexcitation of electrons from neutral centers in the oxide into the conduction band, thus leaving holes trapped at the centers, some trapped holes must be introduced by the last process of Table 4.1. This effect is not observed.

2.4. Summary

In Semi-Annual Report No. 1[25] we reported that in the Si-SiO_2 system the light-induced surface discharge after positive corona charging was dominated by electron photoinjection from the silicon substrate. The photoinjected electrons drifted to the front surface of the insulator where they neutralized the positive charge deposited by the corona ions. Hence the combined corona and photoinjection technique proved to be an effective method for studying the electron injection properties of this structure.

In the present report we have shown that the light-induced surface discharge after negative corona charging is dominated by electron photoinjection from the negative surface charges with subsequent drift of the electrons toward the substrate. The quantum yield of electron photoinjection depends on the surface condition which, in turn, depends on the history of the sample.

Hole trapping was observed when UV light with photon energy corresponding to the minima of R/T was used[25] to discharge samples having high values of electric field ($\sim$ 5 MV/cm). It appears that these holes were

Table 4.1. Results of photodepopulation experiment to determine energy level of the electron traps.

Process / Sample:	V_{FB} (volts)		
	#6	#7	#8
1. Initial	5.85	4.85	5.6
2. Radiated by UV light with photon energy less than 4 eV for 4 hrs.	5.85	4.85	5.6
3. Radiated by UV light with photon energy less than 5.1 eV for 1 hr.	5.5	4.65	5.2
4. Step 3 repeated	5.45	4.45	5.2
5. Radiated by UV light with photon energy less than 6.2 eV for 2 hrs.	4.3	3.7	4.55
6. Step 5 repeated	4.3	3.7	4.4

photoinjected from the substrate. We believe that this experiment has produced, for the first time, evidence for the photoinjection of holes from silicon into silicon dioxide. The quantum yield for hole injection from silicon into thermally grown SiO_2 is at least 3 orders of magnitude smaller than the corresponding yield for electron injection. The small yield, combined with the strong hole trapping near the interface, accounts for the lack of experimental evidence in the past.

Our experiments show that even on SiO_2 samples having good radiation hardness, hole currents can be neglected. This indicates that the density of hole traps near the interface is very high. However, the density of hole traps in the bulk of the oxide is small. Holes transported through the oxide to the interface are trapped, but in radiation-hard samples the position of trapping seems to be so near to the silicon substrate that the trapped holes are able to tunnel almost immediately into the valence band of the silicon, leaving comparatively little trapped charge behind.

We have studied the electron traps generated in silicon dioxide by exposure of the surface to negative corona ions. By means of an etch-off experiment we have shown that the density of these traps is maximum at the front surface and that the concentration decays exponentially inward. The optical depth of the traps is greater than 4 eV, which is considerably larger than the apparent thermal depth of the traps.

3. RECOMBINATION IN THERMALLY GROWN SILICON DIOXIDE

(J. J. Clement collaborating)

3.1. Introduction

Several investigators have noted that the behavior of holes trapped in the thin oxide layer of an MOS structure is considerably different at liquid nitrogen temperature than at room temperature.[39-43] It has been shown that at room temperature the holes generated in oxides exposed to ionizing radiation are mobile, even at relatively low fields.[31,40-46] Thus, it appears that many of the holes generated in the oxide move out of the oxide and pass into the semiconductor (under positive applied bias), but a fraction of the holes are trapped at the $Si-SiO_2$ interface and are responsible for the "permanent" positive charging that is observed.

However, at liquid nitrogen temperature there is evidence that the holes in the oxides are almost immobile for small values of electric field, and thus remain trapped at or near the point where they are generated in the oxide bulk.[40-43]

It has also been known for several years that electrons photo-injected into the oxide can recombine with the trapped holes and hence neutralize the positive charge.[47]

The purpose of this study is two-fold. First, to attempt to measure the cross-section of holes trapped in the oxide for "trapping", i.e., recombining with, electrons injected from the substrate via internal photoemission. Also, we wished to investigate the effect on this cross section of the electric field applied during photo injection. Secondly, we wished to see if we could distinguish between holes trapped at the interface (at room temperature) and holes trapped in the bulk of the oxide (at liquid nitrogen temperatures).

3.2. Experiments

(a) Samples

The samples were n-type (100) silicon with 5-10 ohm-cm resistivity, having an HCl-steam grown oxide with a thickness of about 1000 Å. These oxides are a radiation hardened type developed at RCA. Semi-transparent aluminum gates were evaporated onto this oxide.

(b) Apparatus

The sample chamber can be evacuated with an oil diffusion pump down to pressures in the 1×10^{-6} Torr range. The sample is mounted on the cold finger of a vacuum cryostat, making it possible to cool the sample with liquid nitrogen. The ionizing radiation used to generate holes in the oxide is soft X-ray photons which are generated by accelerating electrons thermally emitted from a heated filament into a molybdenum target held at a 5kV potential. This X-ray generator is also housed in the sample chamber.

The sample chamber is fitted with a fused-silica window for sample illumination. Light for internal photoemission of electrons was provided by a Bausch and Lomb high intensity monochromator with a Xenon arc lamp. A Keithley model 610B electrometer was used to monitor the total injected charge. The charge trapped in the oxide was determined using capacitance-voltage (C-V) techniques, i.e., by monitoring the change in voltage corresponding to a certain value of capacitance. Capacitance measurements were made with a Boonton model 72A capacitance meter operating at 1 MHz.

(c) Procedure

The experimental procedure used to study the recombination of holes with photoinjected electrons is as follows. The experiments were carried out either at room temperature or at a temperature of $83^{o}K$. For experiments at $83^{o}K$ the sample was cooled by liquid nitrogen. The sample was then exposed to X-irradiation with an applied gate bias of + 10.2 V (a gate bias of -10.2 V was used in one experiment). The time of exposure to the X-rays varied from 10-40 sec at $83^{o}K$ to 5-15 minutes at room temperature.

After exposure to X-rays, the initial voltage at the reference capacitance was measured using the Boonton meter. Then a certain positive gate voltage was applied and the sample was illuminated by light with photon energy of $\sim$ 5.1 eV to cause internal photoemission of electrons from the substrate. The magnitude of the gate voltage was changed from one experiment to another in order to study the effect of the electric

field on the cross section, but was in the 6.2 to 20.4 volt range. At various times the light was blocked off and the shift in the reference voltage was measured using the Boonton capacitance meter.

3.3. Theory

For a single trapping cross section, the rate of disappearance of the positively charged holes due to recombination with electrons can be written:

$$-\frac{dp}{dt} = \sigma\, v_{th}\, np \tag{3.1}$$

where n is the density of free electrons in the conduction band, p is the density of trapped holes in the oxide, σ is the capture cross section, v_{th} is the thermal velocity of electrons in SiO_2. Assuming n remains nearly constant, the measured gate current density is given by:

$$j_G = q\, n\, v_d \tag{3.2}$$

where v_d is the drift velocity of electrons in SiO_2. Thus, we can write equation (1) as:

$$-\frac{dp}{dt} = \frac{j_G}{q}\,\frac{\sigma\, v_{th}}{v_d}\, p \tag{3.3}$$

According to the experiments of Hughes,[48] the electron velocity becomes saturated, i.e., v_d is independent of field, for fields above $\sim 5 \times 10^5$ V/cm at room temperature. At liquid nitrogen temperatures this saturation of the drift velocity occurs at even lower fields.[49] Thus, for all of the voltages used in this experiment, the electrons should travel through the oxide at their saturated velocity, $v_{d\,sat}$. Since $v_{d\,sat} \sim v_{th}$,

$$-\frac{dp}{dt} = \sigma\,\frac{j_G}{q}\, p \tag{3.4}$$

Solving this equation:

$$p\,(t) = p\,(t = 0)\, e^{-\sigma N_{inj}} \tag{3.5}$$

where N_{inj} is the total injected charge per unit area measured in the external circuit and is given by

$$N_{inj} = \frac{1}{q} \int_o^t j_G(t')\, dt' \tag{3.6}$$

Now, assuming that the centroid of the trapped charge, $\bar{x}$, remains fixed throughout the experiment, we can write the shift in the reference voltage as:

$$\Delta V_{ref}(t) = V_{ref}(t = 0)\, e^{-\sigma N_{inj}} \tag{3.7}$$

where

$$V_{ref}(t = 0) = \frac{q P_o \bar{x}}{K_{ox} \varepsilon_o}$$

and P_o is the initial effective number of trapped holes per unit area located at $\bar{x}$. Thus:

$$\ln \Delta V_{norm}(t) = - \sigma N_{inj} \tag{3.8}$$

where

$$\Delta V_{norm}(t) = \frac{\Delta V_{ref}(t)}{V_{ref}(t=0)} \tag{3.9}$$

So for trapped holes having a single cross section we should expect a straight line with slope σ when plotting log ΔV_{norm} vs N_{inj}.

The average oxide field E_{ox} is given by

$$E_{ox} = \frac{V_G - Q_s}{t_{ox}} \tag{3.10}$$

where V_G is the applied gate voltage, t_{ox} is the oxide thickness (1000 Å) and Q_s is the potential drop in the silicon substrate. For our samples, with a 5-10 ohm cm substrate, which were biased in accumulation during internal photoemission of electrons, $Q_s \sim .1 - .2$ V which does not have much effect on E_{ox}.

3.4. Results

In order to verify that the initial distribution of holes in the oxide after X-irradiation at 83°K was fairly uniform through the oxide, the following experiment was carried out. The sample, with an applied gate bias of +10.2 volts, was exposed to X-rays for approximately 18 sec. The resulting shift in the reference voltage was 0.289 volts. Electrons were then photo injected into the oxide from the substrate to recombine with the holes with an applied gate bias of +10.2 volt, and the change in the reference voltage monitored. The sample was again exposed to X-rays for approximately 18 sec with an applied gate bias of -10.2 volts. The resulting shift in the reference voltage was 0.259 volt. Once again the change in the reference voltage was monitored as electrons were photo-injected from the substrate into the oxide with an applied gate bias of +10.2 volt.

The normalized change in the reference voltage, ΔV_{norm}, vs the total injected electrons N_{inj}, is plotted on a semi-log graph in Figure 3.1 for both cases described above. It is apparent that the electrons recombine with the trapped holes in an almost identical manner. The difference in the initial shifts in the reference voltage between these two cases can be taken as a measure of the variation from a totally uniform distribution of holes. This variation is on the order of 11%.

It really does not matter whether the initial distribution of holes is uniform or not. What is important is that the centroid of the charge distribution does not change and that at 83°K there are holes trapped in the bulk oxide.

Figures 3.2 - 3.5 show the results for recombination of electrons photoinjected from the substrate with holes trapped in the oxide at 83°K as depicted by a semilog plot of ΔV_{norm} vs N_{inj} for four values of applied gate bias. It is apparent that a straight line asymptote can be fitted fairly well to the data in all cases. The cross section for capture of an electron by a trapped hole is obtained from the slope of this straight line. The results from this type of analysis are given in Table I.

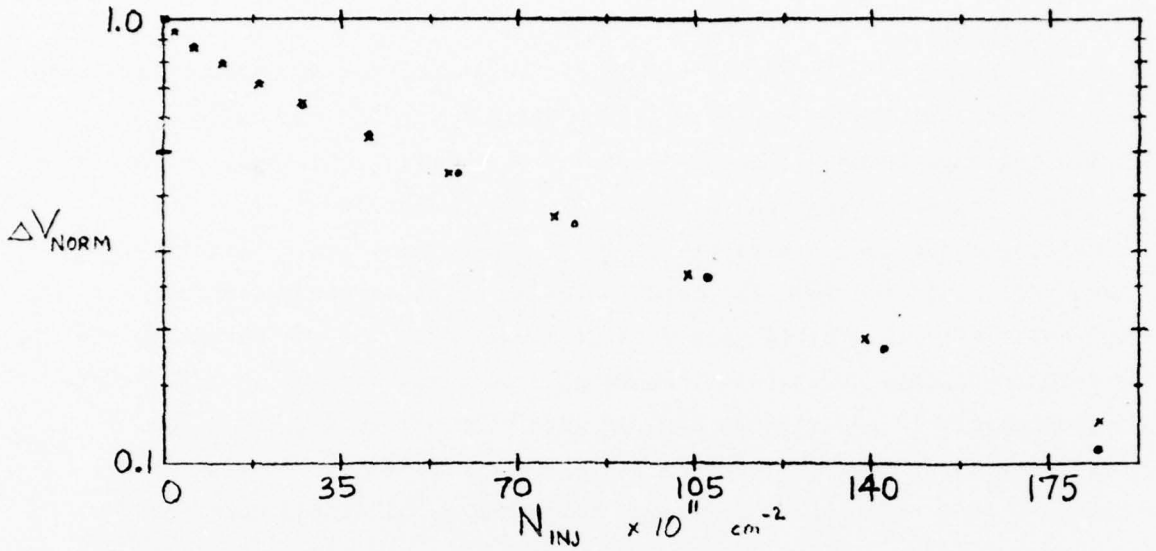


Fig. 3.1. Recombination with an applied gate bias of +10.2 Volts at 83°K.

o - X-irradiation done with +10.2 Volt gate bias; total ΔV_{ref} = .289 Volt

x - X-irradiation done with -10.2 Volt gate bias; total ΔV_{ref} = .259 Volt

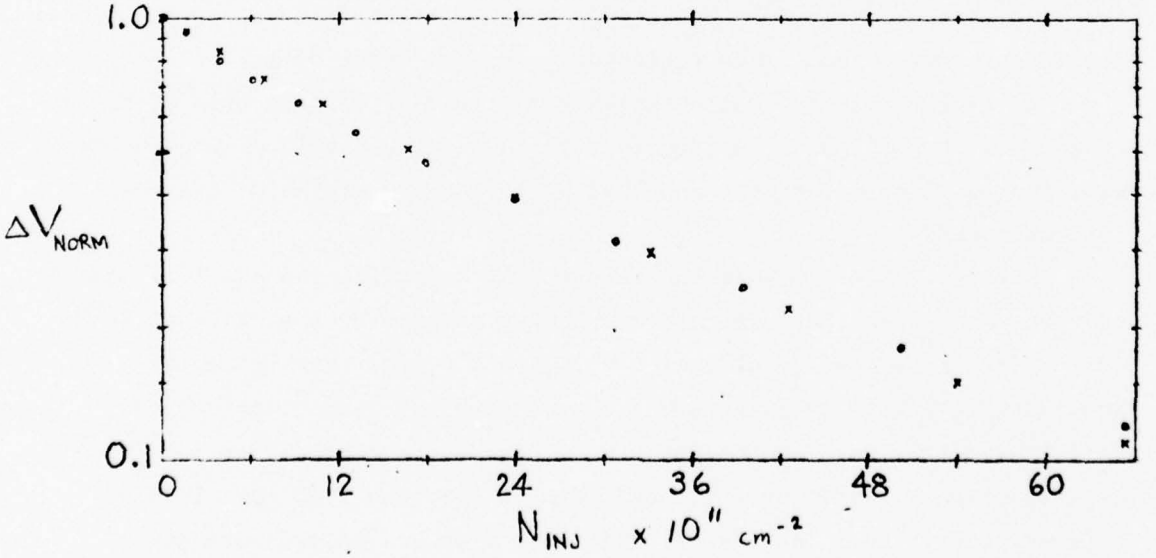


Fig. 3.2. Recombination with an applied gate bias of +6.2 Volts at 83°K for two different samples.

o - 111876 total ΔV_{ref} = .150 Volt

x - 110976 total ΔV_{ref} = .173 Volt

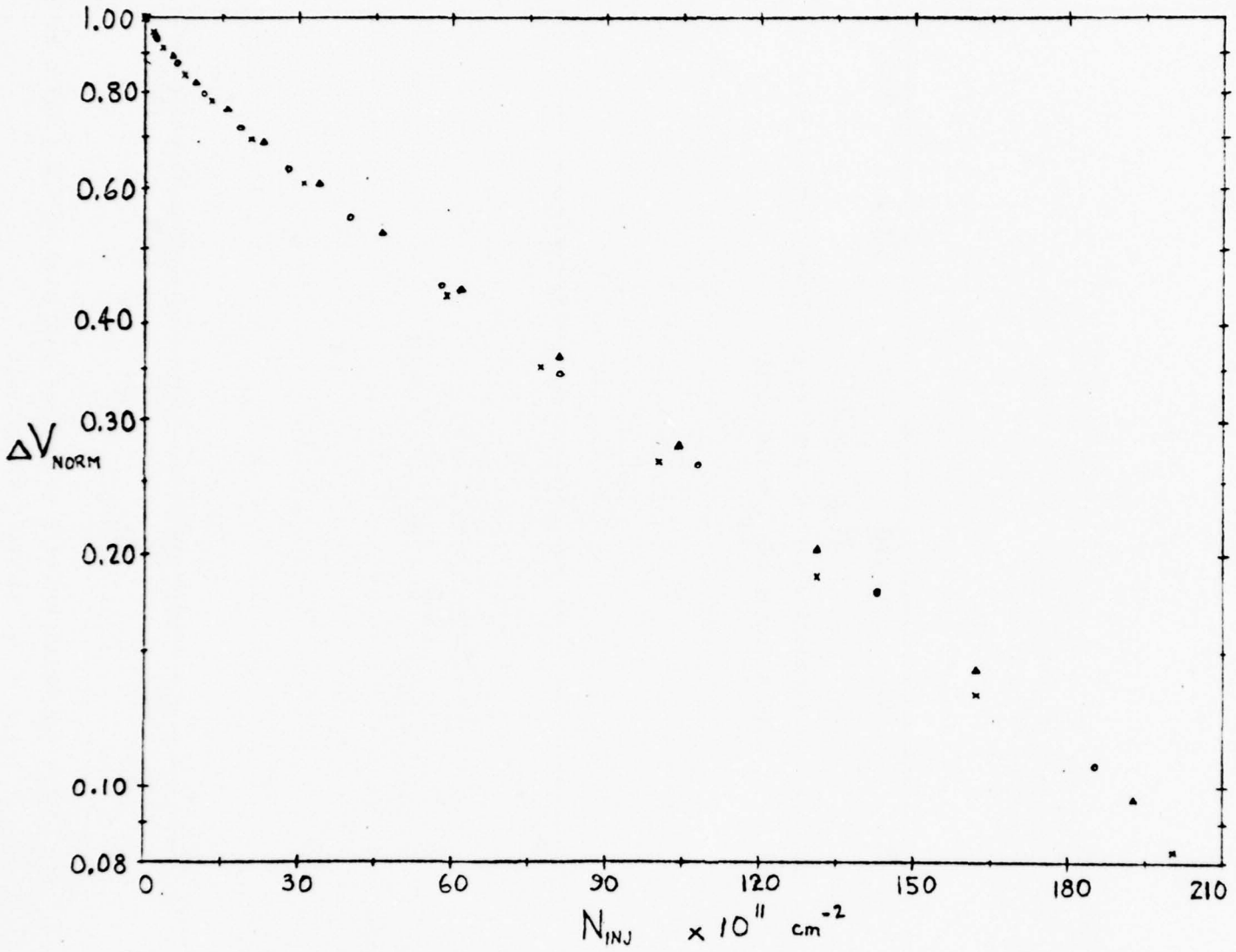


Fig. 3.3. Recombination with an applied gate bias of +10.2 Volts at 83°K for three different samples.

o - 111876 total ΔV_{ref} = .289 Volt
x - 111376 total ΔV_{ref} = .264 Volt
Δ - 110976 total ΔV_{ref} = .253 Volt

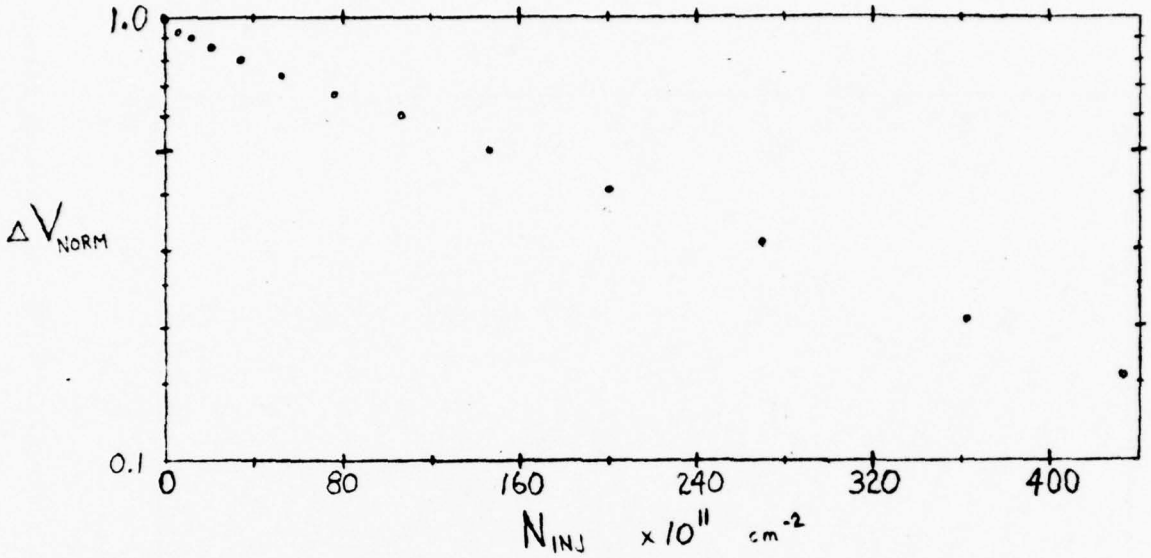


Fig. 3.4. Recombination with an applied gate bias of +15.3 Volts at 83°K. 111376 total ΔV_{ref} = .294 Volt

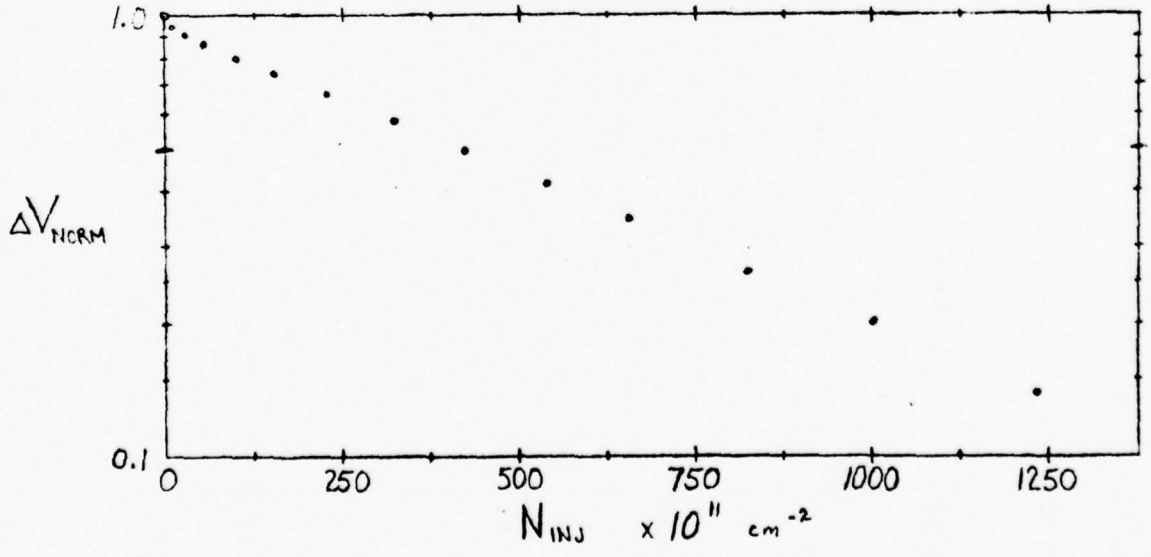


Fig. 3.5. Recombination with an applied gate bias of +20.4 Volts at 83°K. 110676 total ΔV_{ref} = .768 Volt

Table I ($83^{o}K$)

V_G (volt)	E_{ox} (x 10^6 V/cm)	σ (x 10^{-14} cm^2)
6.2	.61	31.23
10.2	1.05	11.89 - 11.17
15.3	1.51	4.09
20.4	2.02	1.53

Figures 3.6 and 3.7 show the results for recombination of electrons photoinjected from the substrate with holes trapped at the interface at room temperature ($300^{o}K$) as depicted by a semilog plot of ΔV_{norm} vs N_{inj} for two values of field. Once again it appears that the data can be fitted well by a single straight line, the slope of which gives us the capture cross section. The results from this type of analysis are given in Table II.

We might mention that there is a significant difference in the amount of exposure to X-irradiation necessary to produce similar shifts in the reference voltage between experiments done at $83^{o}K$ and those carried out at room temperature. This is consistent with the interpretation that most of the holes generated in the oxide at room temperature move out of the oxide with some trapping at the $Si-SiO_2$ interface.

Table II ($300^{o}K$)

V_G (volt)	E_{ox} (x 10^6 V/cm)	σ (x 10^{-14} cm^2)
10.2	1.05	12.23
16.0	1.58	3.81

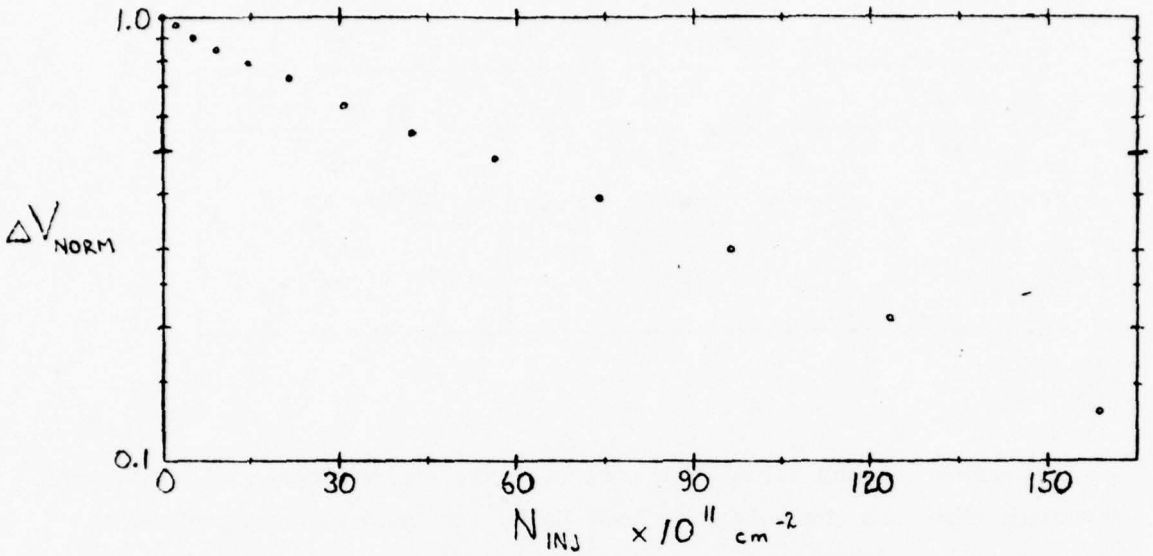


Fig. 3.6. Recombination with an applied gate bias of +10.2 Volts at 300°K.
112376 total ΔV_{ref} = .310 Volt

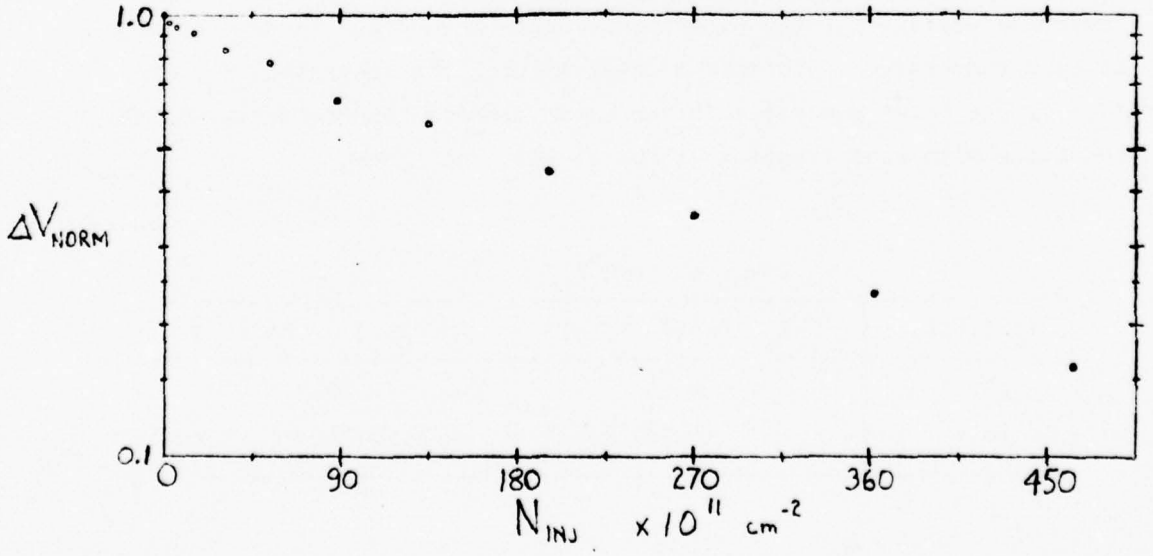


Fig. 3.7. Recombination with an applied gate bias of +16 Volts at 300°K.
112476 total ΔV_{ref} = .282 Volt

3.5. Discussion

The measured capture cross sections from Table I ($83^{o}K$) are plotted vs average oxide field in Figure 3.8. Although there are only four values of oxide field for which we have measured the capture cross section, it appears that at lower fields σ varies approximately as E_{ox}^{-2} while at higher fields this variation of σ approaches $E_{ox}^{-3.5}$. At the present time we have no satisfactory explanation of this behavior of cross section as a function of field.

The measured capture cross sections from Table II ($300^{o}K$) vs the average oxide field are also included in Figure 3.8. It appears that capture cross sections measured at room temperature are practically the same as those measured at $83^{o}K$ (for the same average oxide field) and that the dependence of σ on E_{ox} also does not change much with temperature. This indicates a very weak dependence of the capture cross section on temperature. It also means that we are unable to detect any difference between holes trapped in the bulk at $83^{o}K$ and holes presumably trapped at the interface at room temperature from observation of the manner in which they recombine with photoinjected electrons.

Some special problems were encountered during the course of these experiments. At $83^{o}K$, while trying to measure the capture cross section with a gate bias of +6.2 volt, we found that the number of trapped holes distributed through the oxide must be kept small, i.e., the shift of the C-V curve must be very small. If this condition is not met, one finds that the resulting log ΔV_{norm} vs N_{inj} data plot does not yield a straight line but consistently curves. The reason for this, apparently, is that when the number of trapped holes is too large, this results in a sufficient inhomogeneity in the field through the oxide to have a range of capture cross sections due to large dependence of the capture cross section on the oxide field. Thus, the data for a gate bias of +6.2 volt represents a lower limit on the oxide field for which we are able to resolve the very small voltage shifts of the C-V curve to obtain a capture cross section.

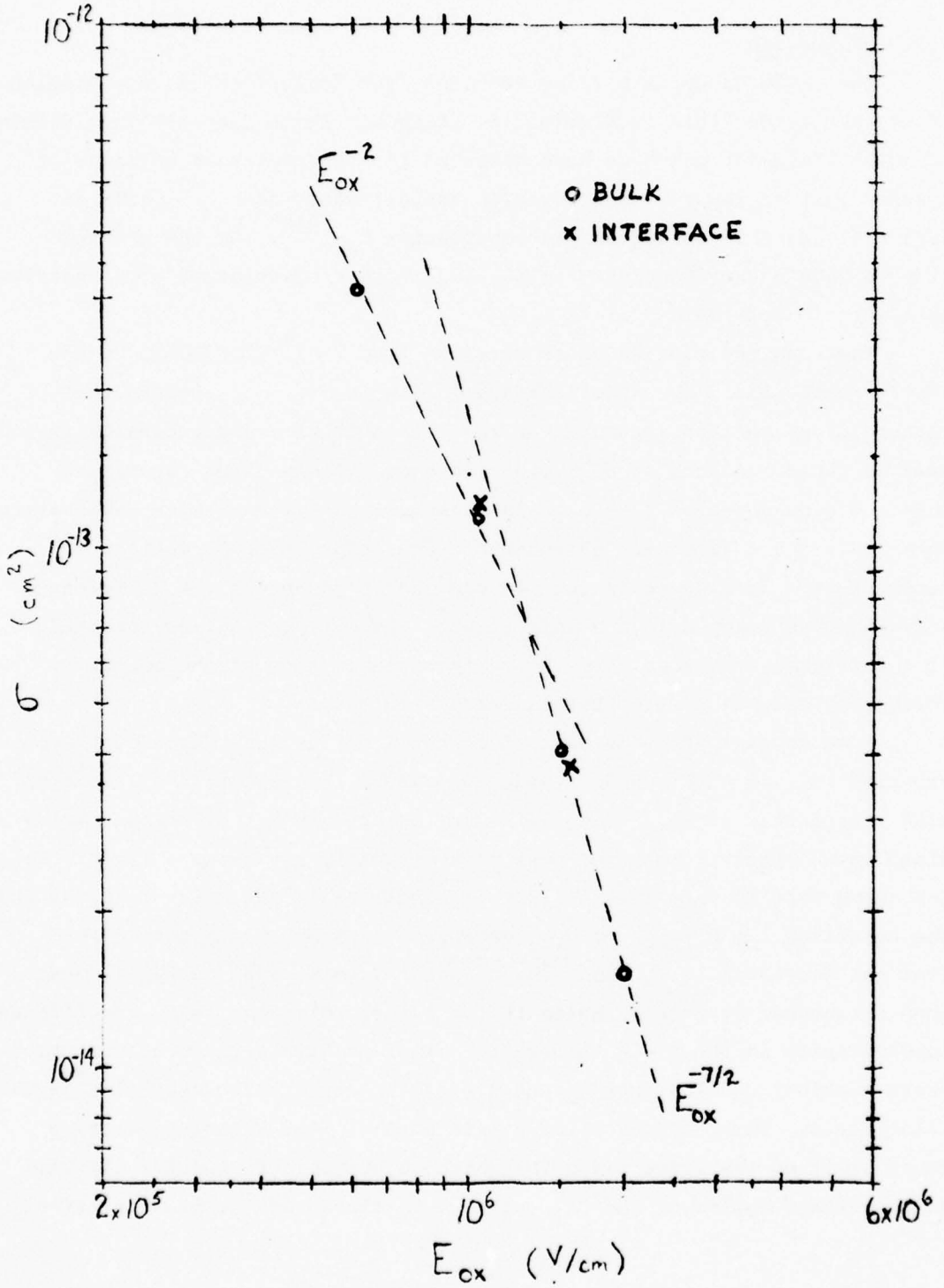


Fig. 3.8. Capture cross sections vs. the average applied oxide field. Circles: 83°K; data taken from Table I. Crosses: 300°K; data taken from Table II.

At the higher fields the capture cross section decreases rapidly due to its large field dependence. Hence, one must photoinject many more electrons to obtain the same change in ΔV_{norm} as compared to internal photoemission at the lower fields. The method used in these experiments (internal photoemission of electrons from the substrate using a Xenon lamp with a monochromator as a light source) as well as relative position of the sample to the light source, results in a certain photoinjection current which cannot be increased. Thus, for an oxide field of 2×10^6 V/cm it takes 9-12 hrs to complete an experiment. At higher fields it would take even longer, since the capture cross section goes at least as E^{-3} (an optimistic guess at $E_{ox} \sim 2.5 \times 10^6$ V/cm would be 17.6 hr). It is apparent that it quickly becomes unfeasible to gather much data at higher fields.

There is one final observation which we note. In every experiment, after the sample is exposed to X-irradiation and the trapped holes recombine with electrons photoinjected from the substrate, the reference voltage eventually shifts to the <u>right</u> of the initial reference voltage before X-irradiation. This shift in the positive direction indicates either a generation of acceptor-like interface states or additional trapping of electrons. At room temperature, X-irradiation causes a large amount of stretch-out of the C-V curve. However, the recombination of photoinjected electrons with trapped holes causes a nearly parallel shift in the C-V curve to the right. This indicates that reason for the shift of the reference voltage past its pre-irradiation value (which is considerable) is due largely to the generation of interface states.

At $83^{\circ}K$ the amount of stretch-out of the C-V curve after X-irradiation is negligible, and the amount by which the reference voltage shifts past its pre-irradiation value is very small. The magnitude of this shift is larger for experiments carried out at higher fields, which require longer times and more total injected electrons to complete. Thus, it is unclear whether this small shift in the reference voltage to the right of its original position is due to the slow generation of interface states at $83^{\circ}K$ or due to slow trapping of electrons.[50-55] The dependence of interface

state creation on temperature and time, as well as the number of holes at the interface, applied bias, and other factors is a topic which requires further research.

3.6. Summary

We have measured the cross section for capture of electrons injected via internal photoemission from the substrate with holes trapped in the oxide at $83^{o}K$ for four values of oxide field. The variation of the capture cross section with oxide field gives an E^{-2} dependence at low fields, approaching a $E^{-3.5}$ dependence at higher fields.

We have measured the capture cross section for recombination of holes trapped at the interface at room temperature for two values of oxide field. We observe no significant variation in the behavior of the capture cross sections from that obtained at $83^{o}K$. This indicates a very weak dependence of the capture cross section on temperature. In addition, we fail to distinguish any difference between holes trapped in the oxide bulk and those trapped at the $Si-SiO_2$ interface by observation of the manner in which they recombine with photoinjected electrons. This result is contrary to our original expectations.

4. HIGH-FIELD CREATION OF ELECTRON TRAPS IN SILICON DIOXIDE

(C. Jenq collaborating)

4.1. Introduction

We have found during the study of the effect of high electric fields on the interface properties of metal-silicon dioxide-silicon structures that electron traps were created after the sample was subjected to a field of 7.2×10^6 V/cm at the temperature of 87°K. No electron traps were found for a sample to which was applied a field of 6.7×10^6 V/cm. The threshold field which starts the onset of the creation of the electron traps is thus expected to be between 6.7×10^6 V/cm and 7.2×10^6 V/cm.

Some of the properties of the traps will be given in this report.

4.2. Experiments

The samples used were RCA HCl-steam grown silicon dioxide films with thicknesses of about 1980 Å and 980 Å. The substrates were n-type silicon. The front contacts of the capacitors were semi-transparent Al gates.

The experimental set-up enables the samples to be cooled down to 87°K. A high field was applied to the sample from a regulated power supply via a voltage divider. The sample can be exposed to a UV light source through a window. The application of high-field bias and the internal photoinjection were both done at $86\text{-}89^\circ$K.

4.3. Results

(4.3a) Initial Electron Trap Concentration

The initial electron trap concentration for a fresh sample was checked by internal photoinjection of electrons from either the metal gate or the silicon bulk at 87°K. The results are shown in Fig. 4.1. The shifts of the C-V curves were 0.05 V for the 980 Å oxide and 0.1 V for the 1980 Å oxide. The corresponding number of trapped charges is at most 1.1×10^{10} cm^{-2} for either oxide.

(4.3b) Electron Traps Created by the High Field

Figure 4.2 gives an example of the effect of high fields on the sample with 1980 Å oxide. Curve 1' and curve 1 are the initial high-frequency CV curves for temperatures of 66°C and 87°K respectively. A voltage of 142 V was applied (7.18×10^6 V/cm) for 1 hr.

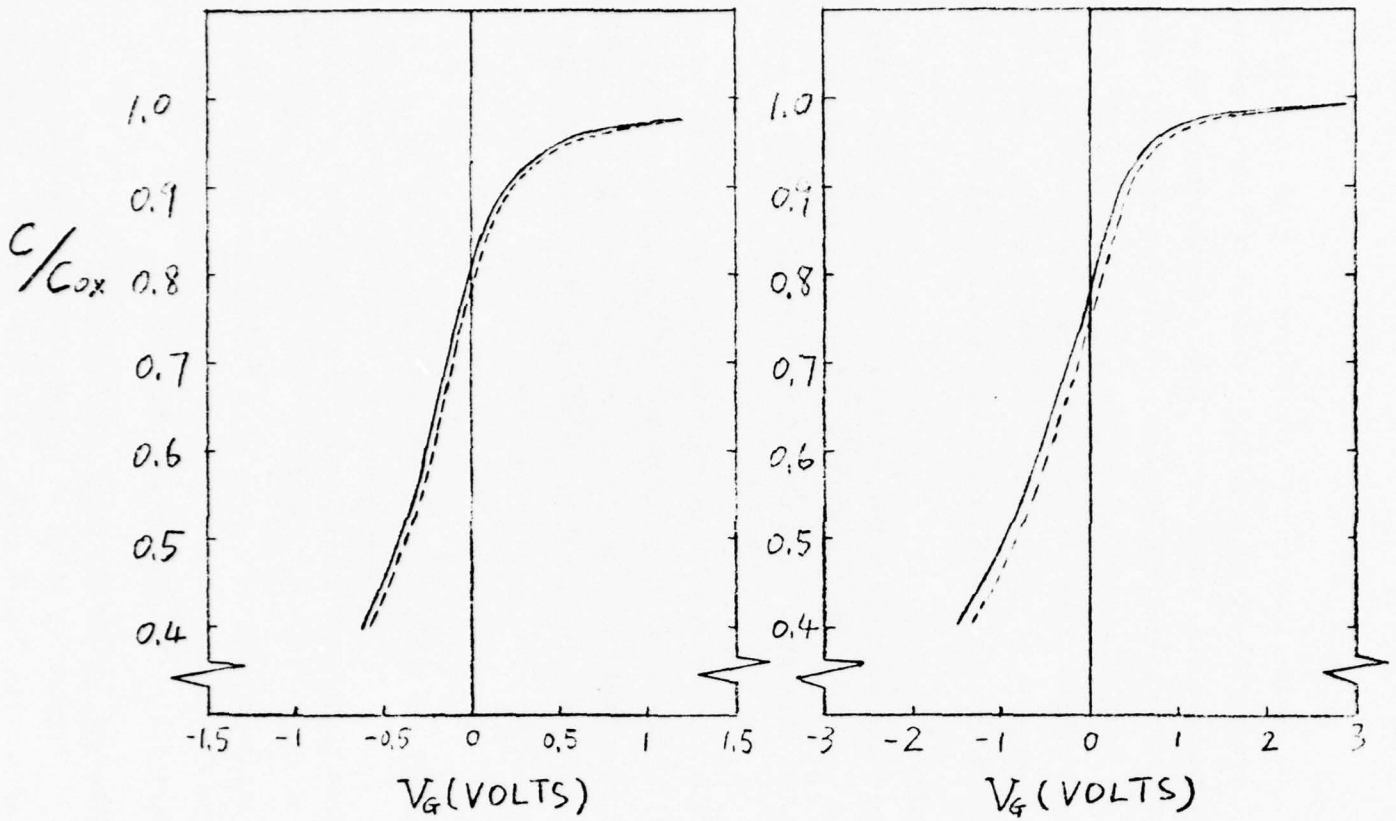


Fig. 4.1. (a) —— Initial 87°K CV for a sample with 980 Å oxide.
---- After 60 min of internal photoinjection from metal gate. (4 eV light, gate bias = -2.85 V).

(b) —— Initial 87°K CV for a sample with 1980 Å oxide.
---- After 60 min of internal photoinjection from Si bulk. (4.8 eV light, gate bias = +5 V).

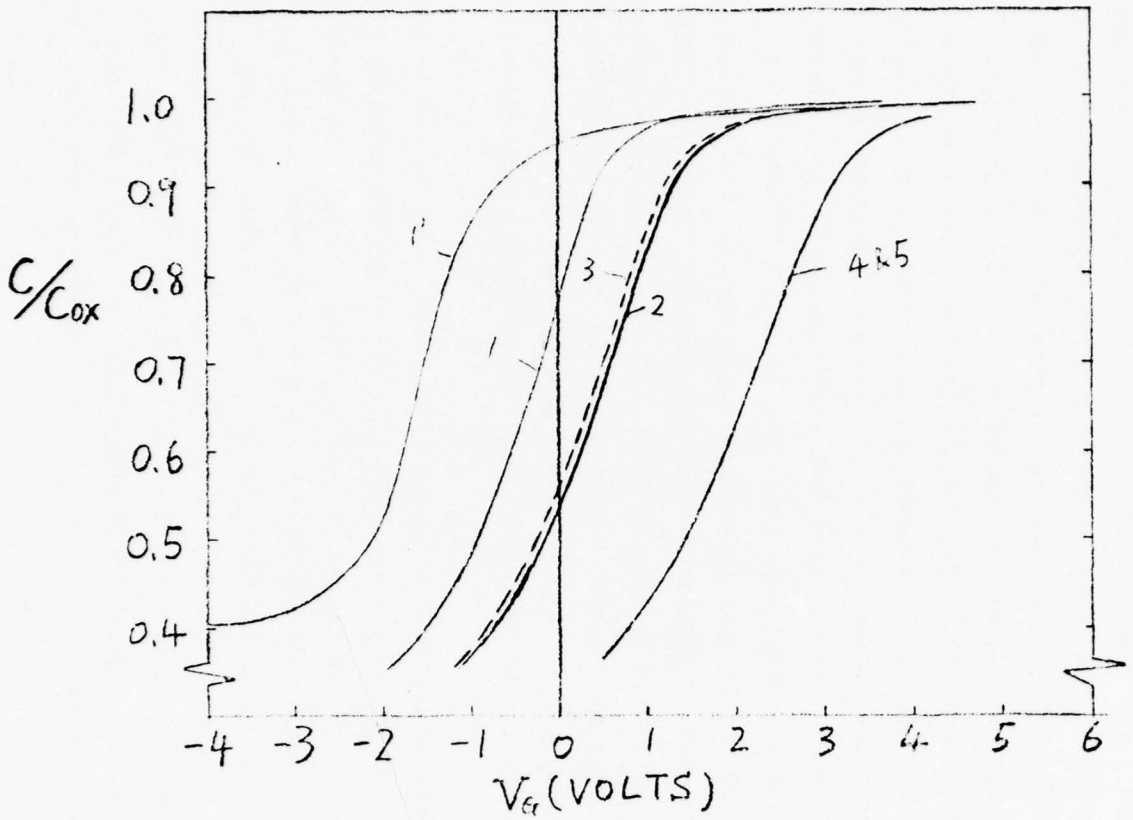


Fig. 4.2. (1') Initial CV at 66°C for a sample with 1980 Å oxide.
(1) Initial CV at 87°K.
(2) After being biased at 142 V (7.18 x 10^6 V/cm) for 1 hr.
(3) After 4 eV light irradiation with gate biased at 5 V for 30 min and another 30 min.
(4) After internal photoinjection (4.8 eV light, gate bias = 5 V) for 30 min.
(5) After 50 min of 4 eV light irradiation with 5 V gate bias.

The effect of this treatment is to shift the C-V curve from 1 to 2. The positive shift indicates negative charging of the oxide. The sample was next biased at 5 V in the dark for 30 min. The resulting C-V curve was almost exactly the same as curve 2. This indicates that the negative charges introduced in the oxide by the high field treatment are not mobile under the 5 V bias. The sample was then exposed to light with a photon energy of 4 eV with the metal gate biased at 5 V. After 30 min of this treatment, curve 3 was obtained. The treatment was then repeated for an additional 30 min. Curve 3 was again obtained. This suggests that 4 eV UV light can depopulate only a small fraction of the trapped charges.

Electrons were then injected from the silicon bulk by exposure to 4.8 eV light with the metal gate still biased at 5 V. Curve 4 was obtained after 30 min of this internal photoinjection. The positive shift of curve 4 from curve 3 indicated that some of the injected electrons were trapped. Efforts were made to depopulate the trapped electrons by 4 eV light with the gate biased positive. After 50 min of the attempted photodepopulation, curve 5 was obtained, which is exactly the same as curve 4. This shows that the trapped charges cannot be photodepopulated by 4 eV light.

Three possible mechanisms of negative charge trapping can be devised to explain the C-V shifts in Fig. 4.2: (1) Acceptor-like electron traps were created after the sample was biased at a high field. The traps were neutral at first but became negatively charged when they trapped the electrons which were injected into the oxide. (2) Instead of the electron traps, acceptor-like hole traps were created. These traps were neutral at first, but became negatively charged when the holes were removed from the traps either by photodepopulation or by high field tunneling. (3) Interface states were created during the process of internal photoinjection.

The third mechanism will be ruled out by the discussion in section 4.3(c). Furthermore, the second mechanism is shown to be impossible from the result of the following experiment:

A sample was first high-field treated, and electrons were then injected from the metal gate by 4 eV light with the gate biased negatively. Curve 3 in Fig. 4.3(a) showed a resulting C-V shift. Comparing the shift ΔV_{a2} in Fig. 4.3(a) to that between Curves 2 and 3 in Fig. 4.2, it is clear that the negative charging is due to the trapping of electrons instead of the depopulation of the holes, for the latter process should give the same result in both cases.

(4.3c) The Role of the Trapped Charges on the Formation of the Interface States

In order to see the effect of the trapped electrons (from internal photoinjection) on the formation of the interface states, the following experiment was carried out.

A voltage of 142 V (7.18×10^6 V/cm) was applied simultaneously to two adjacent samples having an oxide thickness of 1980 Å. The time of application was 50 min. Both samples were then exposed to 4 eV light for 40 min and 4.8 eV light for 6 min with the metal gate of one sample (Sample a) biased at -5 V and the gate of the other (Sample b) at 0 V. Curve 3 in both Fig. 4.3(a) and Fig. 4.3(b) shows the results. The small value of ΔV_{b2} is due to the fact that Sample b was biased at 0 V, so that the initial field at the interface was too small to give significant injection.

The sample was then warmed up to 66°C, and the high-frequency C-V curves were taken. These are shown in Fig. 4.4 as Curve 1a (for Sample a) and Curve 1b (for Sample b). Curves 1a and 1b are almost parallel. This indicates that the surface-state densities for the two samples are nearly the same. Calculation confirmed this statement (Fig. 4.5).

The foregoing provides evidence that neither the process of internal photoinjection nor the trapped electrons themselves introduce additional surface states. This rules out the third mechanism in Section 4.3(b). The flat-band voltage difference ΔV_c is thus attributed to the trapped electrons in the oxide.

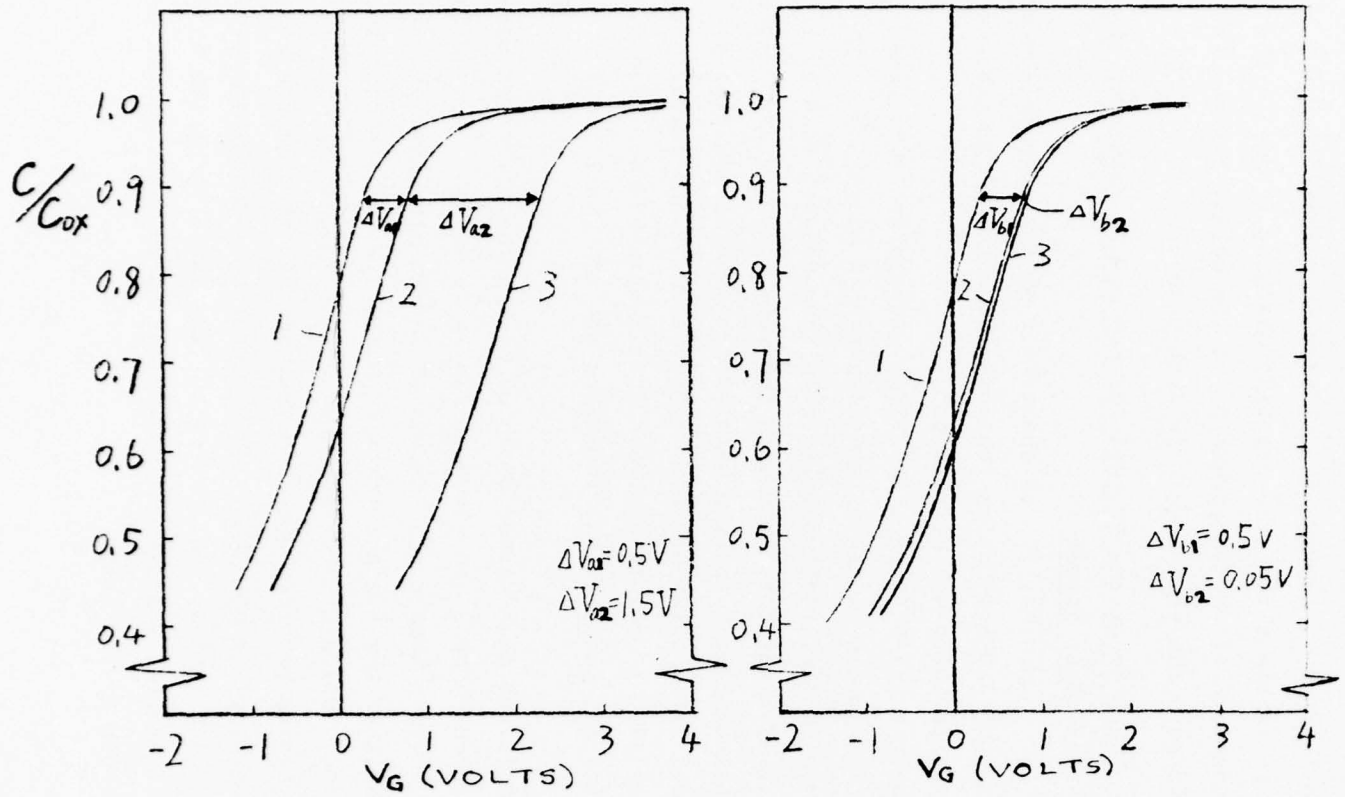


Fig. 4.3. (a) 1. Initial 87°K CV for Sample a with 1980 Å oxide.
2. After being biased at 142V (7.18×10^6 V/cm) for 50 min.
3. After internal photoinjection from metal gate by 4.8 eV light for 6 min and 4 eV light for 40 min with gate biased at -5V.

(b) 1. Initial 87°K for Sample b with 1980 Å oxide.
2. After being biased at 142V (7.18×10^6 V/cm) for 50 min.
3. After irradiation of 4.8 eV light for 6 min and 4 eV light for 40 min with gate biased at 0 V.

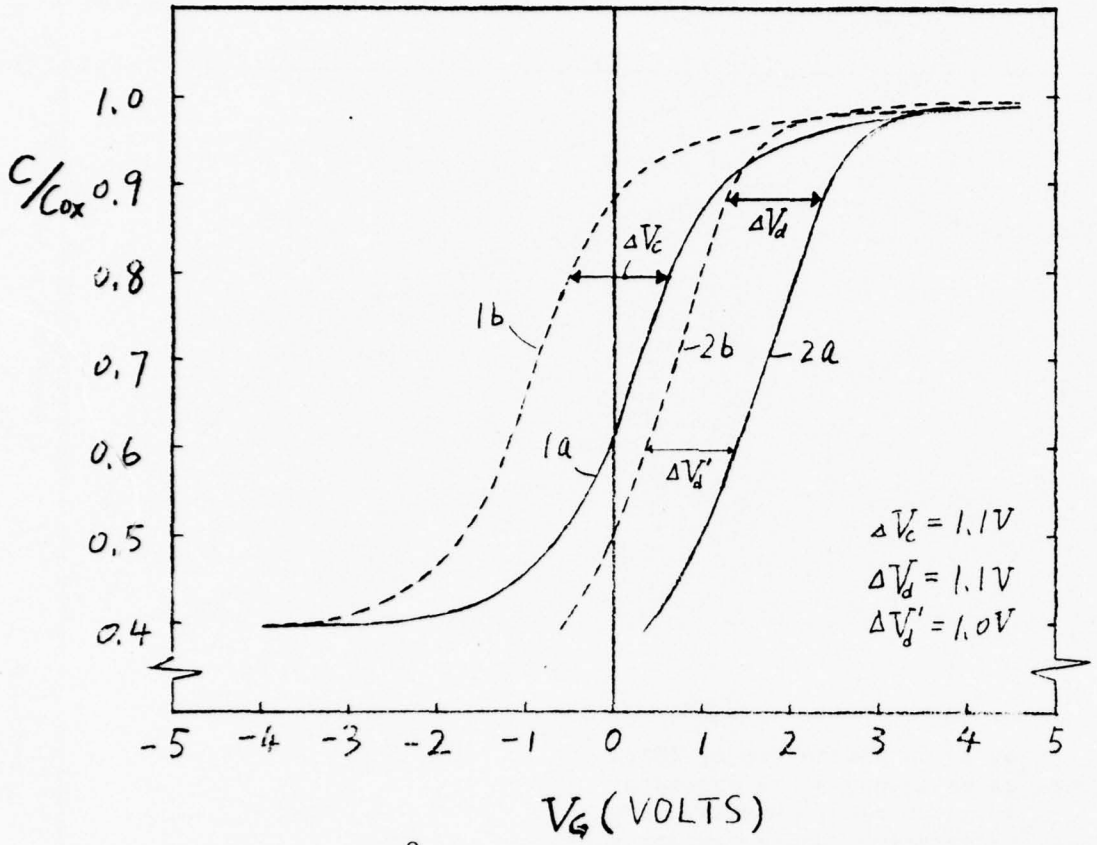


Fig. 4.4. (1a) 66° C-V curve for Sample a after it was warmed up from the state of curve 3 in Fig. 3(a).
(1b) Same as the above for Sample b.
(2a) 87°K C-V curve for Sample a when it was cooled down again.
(2b) Same as the above for Sample b.

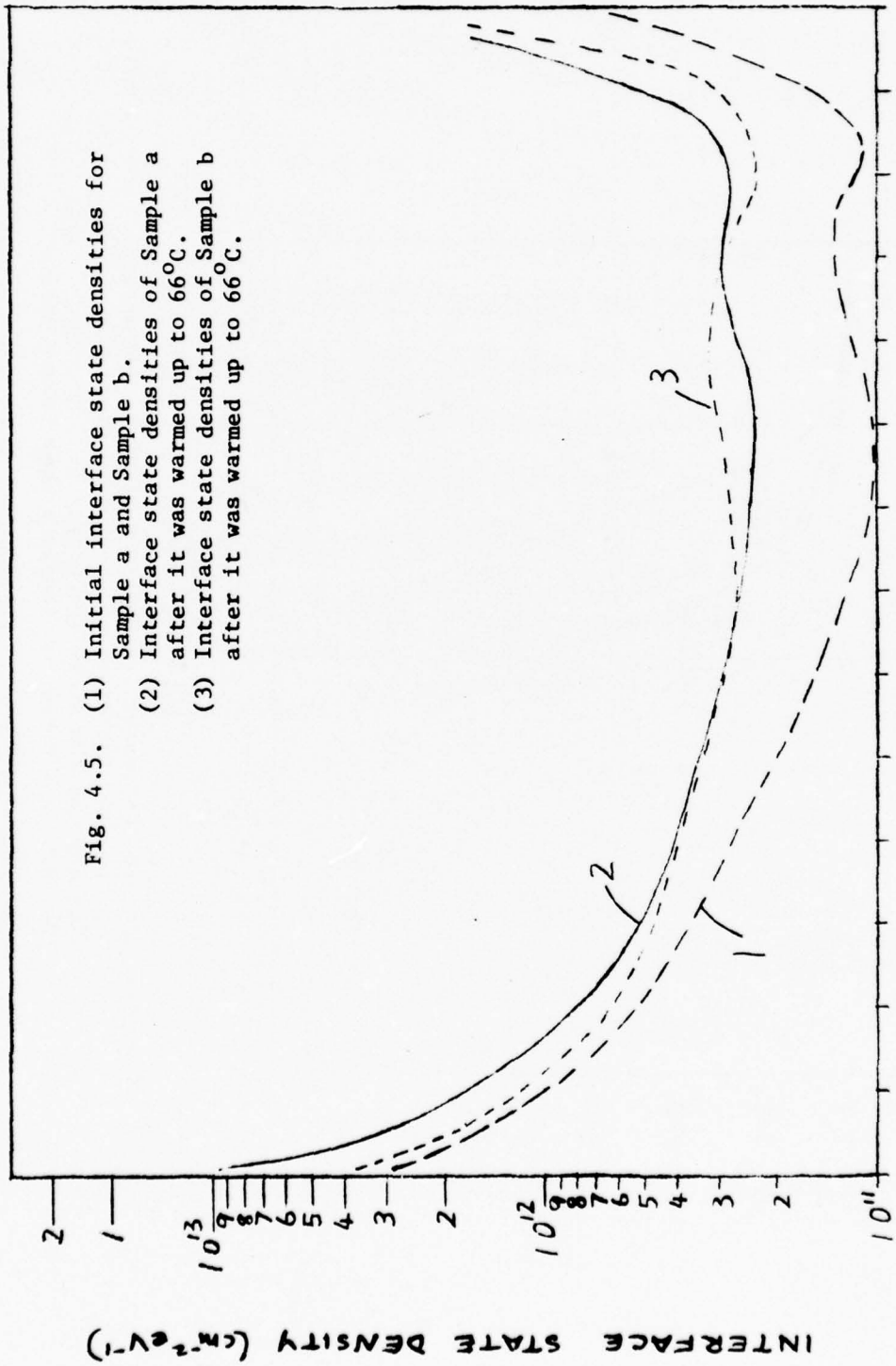


Fig. 4.5. (1) Initial interface state densities for Sample a and Sample b.
(2) Interface state densities of Sample a after it was warmed up to 66°C.
(3) Interface state densities of Sample b after it was warmed up to 66°C.

It is interesting to notice that ΔV_c (1.1V) is only 0.35 V less than the difference between ΔV_{a2} and ΔV_{b2} (1.5 V - 0.05 V = 1.45 V). This suggests that only about 24% of the trapped electrons were removed during the warming up process.

Curves 2a and 2b in Fig. 4.4 were obtained after the samples were cooled down to 87^{o}K again. The shift between 2a and 2b is, as it should be, about the same as ΔV_c.

4.4. Conclusions

Our study of high-field effects in HCl-steam grown silicon dioxide films shows that acceptor-like electron traps are created in the oxide at fields of approximately 7 x 10^6 V/cm. The negative charging of these traps is shown to have no significant effect on the formation of interface states. Additional studies of the electron traps are currently underway with the objective of characterizing the properties of the traps.

5. HIGH-FIELD CHARGING AND BREAKDOWN OF Al_2O_3.

(O. Bar-Gadda collaborating)

As part of a continuing investigation of dielectric breakdown mechanisms in technologically important insulators, we report here on some recent studies of Al-Al_2O_3-Si capacitors.

The substrate was p-Si of 4-6 cm resistivity. A 450 Å film of Al_2O_3 was grown by chemical vapor deposition at a temperature of 900°C, and Al dots of 1000 Å thickness and diameters of about 500 μm were deposited on the Al_2O_3 film. An Al back contact was also deposited on the Si substrate.

Experiments were performed to determine the high-field charging characteristics of the insulator. A negative bias was applied to the Al field plate, and the flatband shift ΔV_{FB} of the C-V curve was measured at uniform intervals in time. The average applied field was varied from 2 to 7 MV/cm. We show typical C-V traces for the cases of low and high fields (Figs. 5.1 and 5.2). The increasing shift to the right (positive flatband shift) of the various C-V curves indicates that the initial charging is probably dominated by electron injection from the metal electrode and trapping in the oxide near the metal. An order-of-magnitude calculation based on a unform trapping distribution gives an estimate of $n_t = 2 \times 10^{19}$ cm^{-3} for the density of electron traps.

We plot the flatband shift vs. log time for different applied voltages in Fig. 5.3. Note that the initial behavior approximates a $\log(1 + t/t_o)$ dependence, but that, for large t, V_{FB} apparently saturates. This time dependence has been noted before for Al_2O_3, and can be used in conjunction with current(I)-time(t) plots to yield a true I-V curve.

The initial charging characteristics are studied here to provide data on trapping and injection mechanisms. Dielectric breakdown does not appear to take place during this process, however. To study breakdown, we must apply a high enough bias for times longer than the time required to reach the initial saturation in the C-V curve.

Figure 5.4. shows the result of such an experiment carried out at a field of 5.5 MV/cm. The first curve taken at t = 10s shows both a

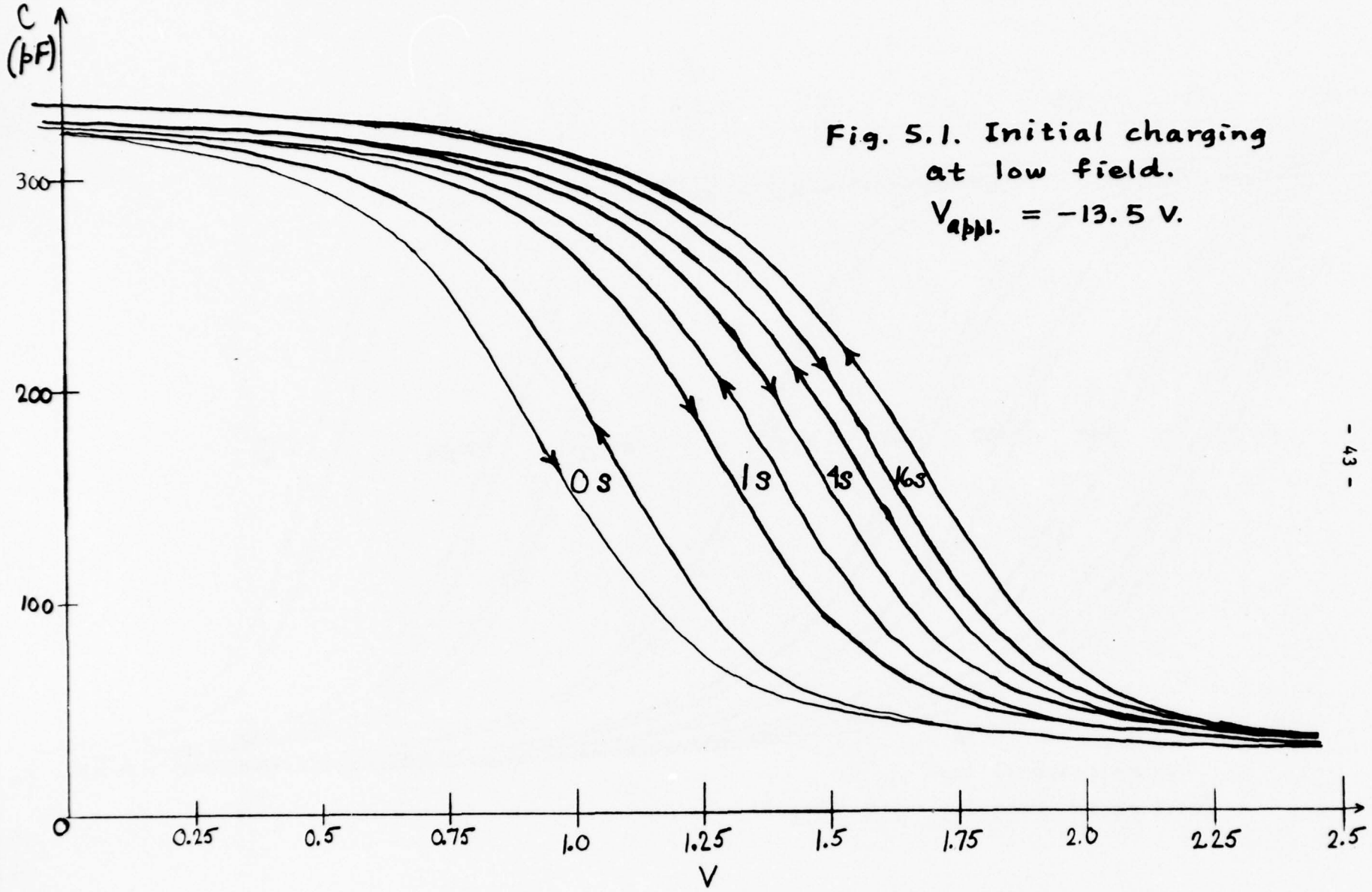


Fig. 5.1. Initial charging at low field.
$V_{appl.} = -13.5$ V.

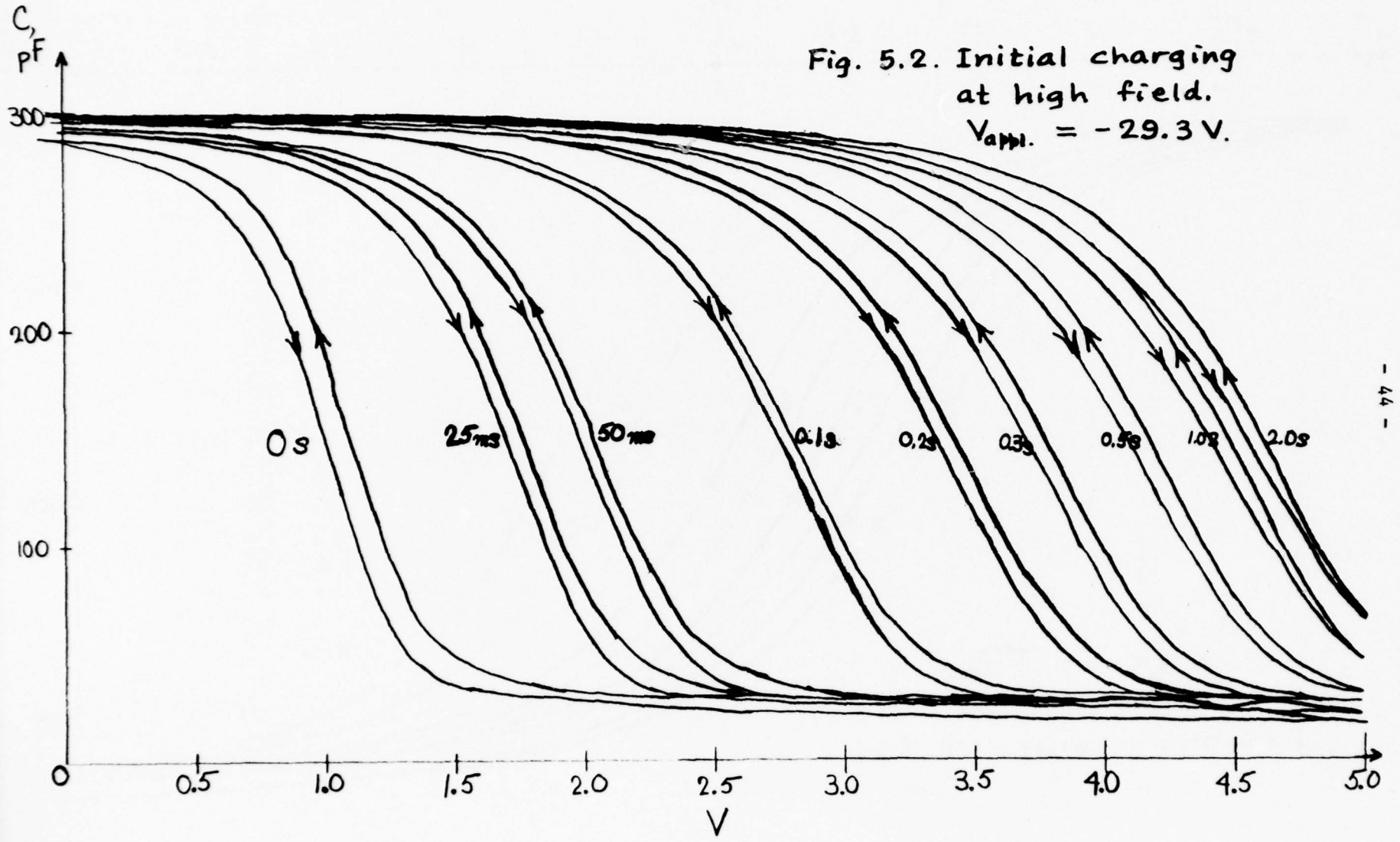


Fig. 5.2. Initial charging at high field.
$V_{appl.} = -29.3$ V.

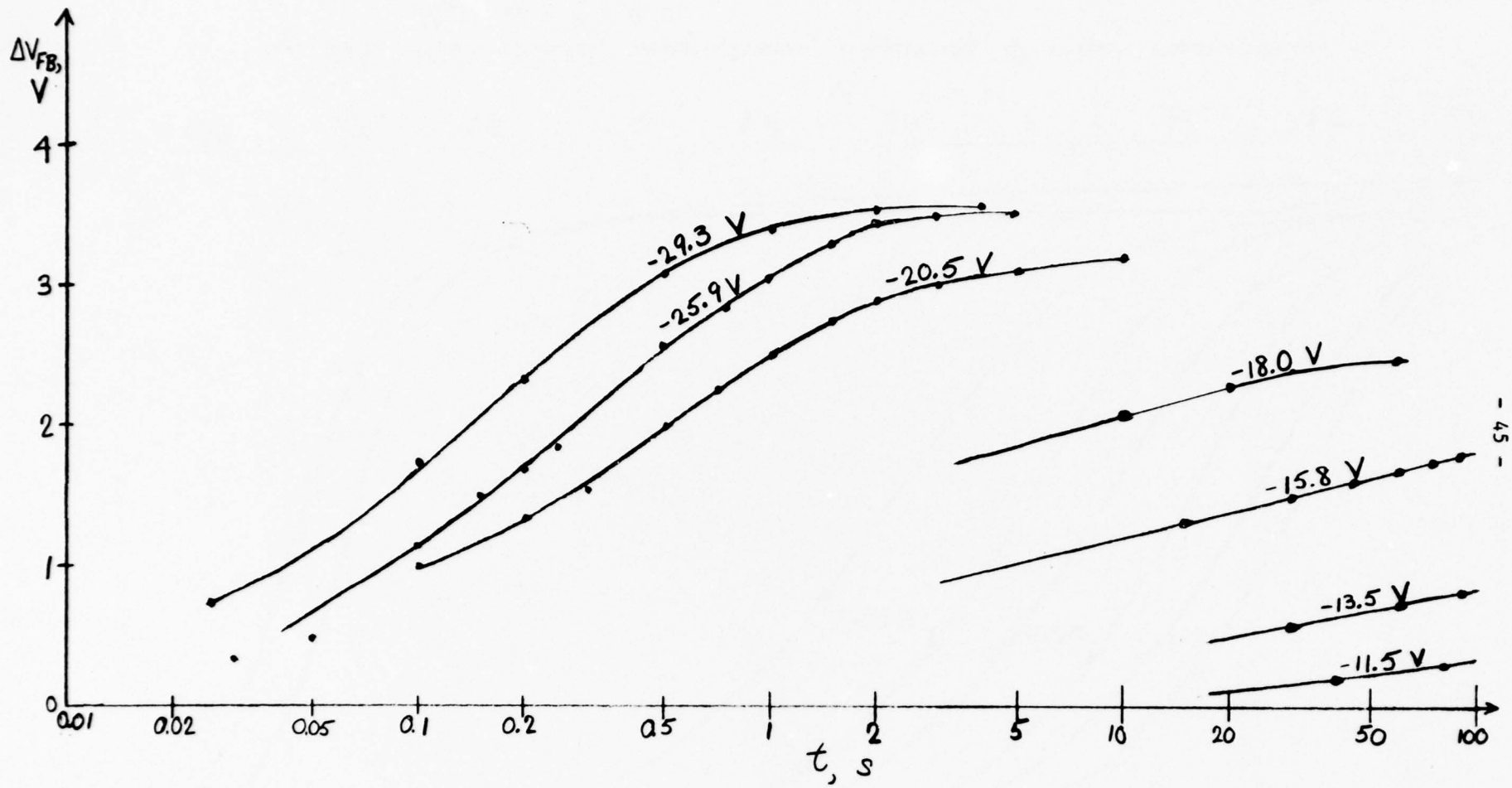


Fig. 5.3. ΔV_{FB} vs. log t for different fields.

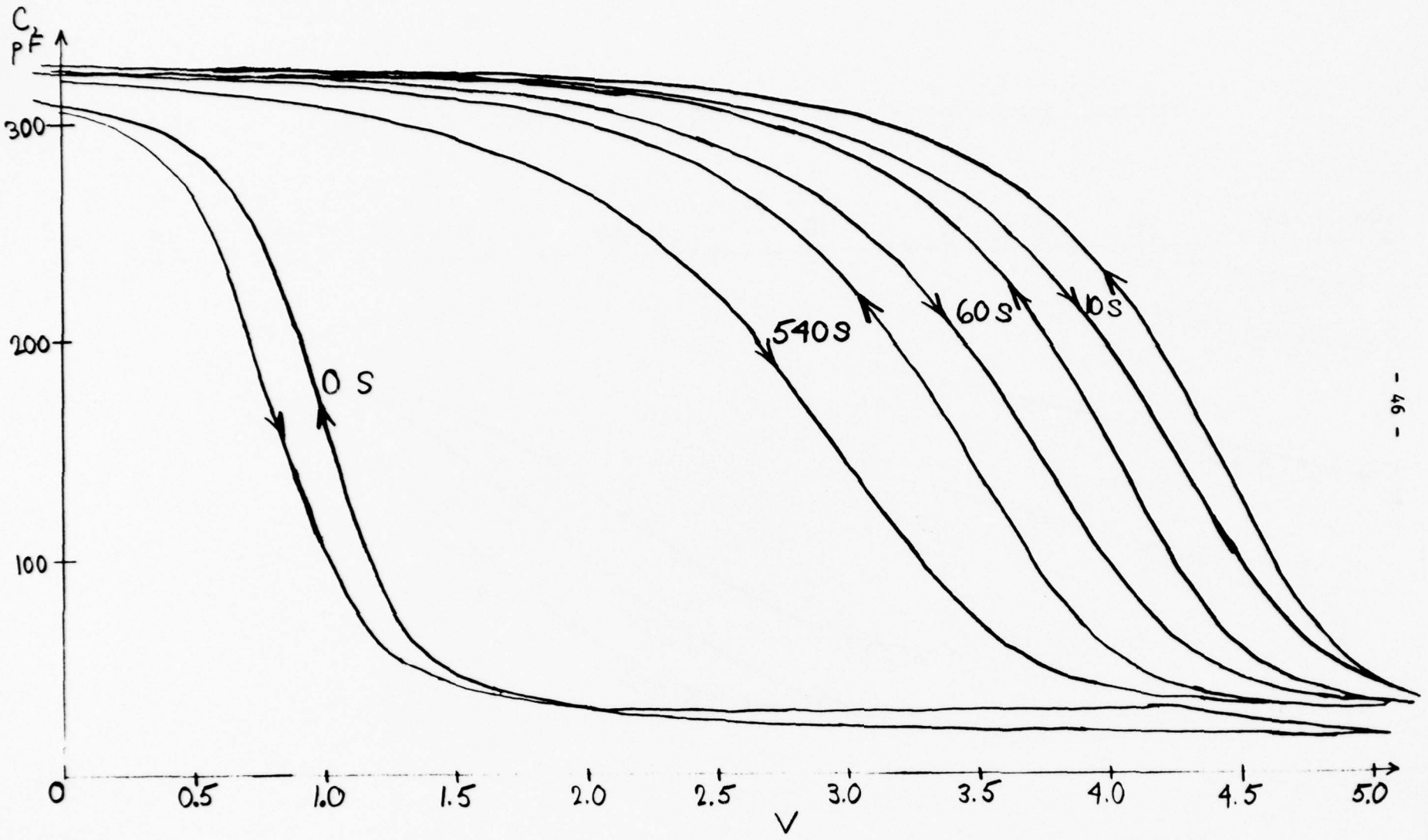


Fig. 5.4. High-field, long-time, negative charge reduction.
$V_{ABM.} = -24.8$ V.

flatband shift and an appreciable stretchout of the C-V curve. Actually one observes this stretchout in the initial charging curves (Figs. 5.1, 5.2). This is due to the creation of interface states at the Si-Al_2O_3 interface and/or the presence of lateral nonuniformities in the oxide charge distribution. The main feature of this curve is that, as time goes on, the C-V curve shifts to the left. This reduction in negative charge might be due to hole trapping and/or electron detrapping. Further work to determine the nature of this shift is planned. At a higher field, 5.8 MV/cm, the sample apparently "broke down" during this period. That is, while the bias was on, the current through the sample suddenly jumped to a value several orders of magnitude higher than before, after monotonically decaying. The sequence of events was as follows. The field (5.8 MV/cm) was applied to the sample, and the current through the sample was monitored. The current showed an initial jump following application of the step voltage, and then monotonically decayed. Then, after a few seconds, the current very suddenly jumped by several orders of magnitude. Simultaneously, the voltage across the sample dropped. The voltage/current ratio indicated that the resistance had decreased to about 40 kΩ. However, the sample was apparently not destroyed, because we were able to trace out a C-V curve. This high-conduction state seemed, however, to be of a permanent nature. Attempts to reapply the same high bias only resulted in the same state of high conduction. We observed, however, that leaving the sample in this high-conduction state caused a continued positive C-V shift as well as a reduction in the stretchout of the C-V curves. We do not yet have enough data to offer a model for this phenomenon.

6. HIGH-FIELD STUDIES OF ALUMINUM OXIDE FILMS

(S. S. Li collaborating)

6.1. Introduction

Powell and Hughes[56] observed that an Al_2O_3 MOS structure under positive bias with a field of approximately equal to 1.5 MV/cm in the oxide will have electron injection from the substrate into the oxide. Also, there will be a considerable amount of electron trapping in the oxide, giving rise to a positive flatband shift. It was noted by Walden[57] that the flatband shift is a linear function of log time.

Powell and Hughes[56] also observed that if the Al_2O_3 MOS structure is biased negatively, there is only a small positive flatband shift. This may be caused either by a significant amount of electron trapping near the Al-Al_2O_3 interface or to a more limited amount of electron trapping in the bulk of the Al_2O_3.

In our experiments we applied high fields to the Al_2O_3 by two different methods: (1) by biasing a metallic field plate negatively and (2) by negative corona charging of the unmetallized surface. Our results show a stretch-out of the C-V curves which can originate from either the creation of interface states or from lateral nonuniformities in the stored charge. In the following section, we report our investigation of this phenomenon.

6.2 Experimental Results

(a) Charging the Sample by Corona

Two kinds of samples were used in the corona-charging experiment. The first, supplied by Bell Laboratories, had an n-type (100) silicon substrate with 4-6 Ω-cm resistivity and a pyrolytic film of Al_2O_3 with thickness 450 Å. The second type of sample, fabricated by RCA Laboratories, had a (100) silicon substrate with 8-12 Ω-cm resistivity and a pyrolitic Al_2O_3 film with a thickness of 1000 Å.

Figure 6.1 shows the results of a corona-charging experiment on a Bell Laboratories (BL) sample of aluminum oxide. It is seen that exposure

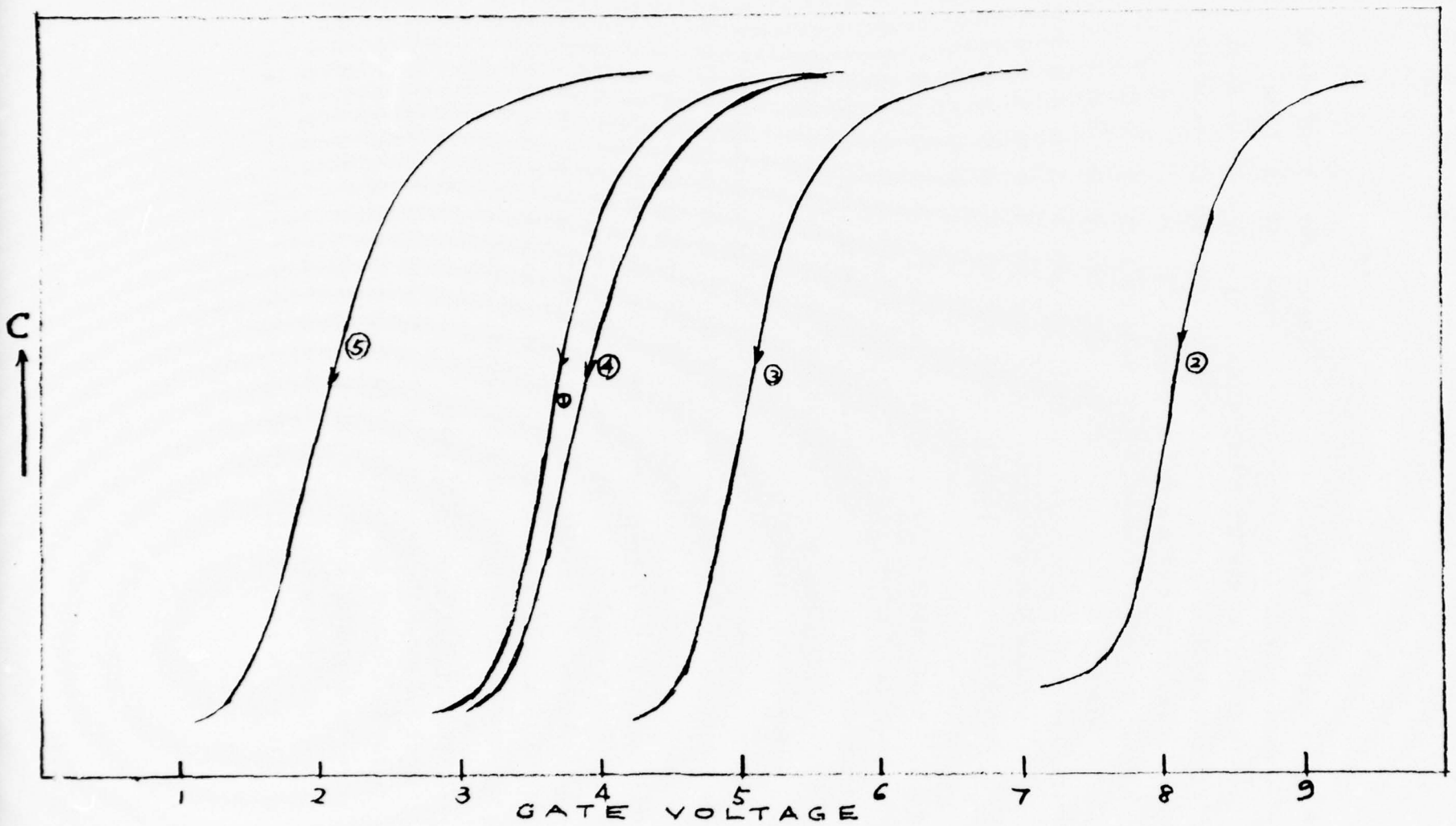


Fig. 6.1. Results of corona-charging experiment on BL sample of Al_2O_3. (1) Fresh sample. (2) After positive corona, 6×10^{-7} A/cm^2, 3.5 min. After negative corona; (3) 9×10^{-8} A/cm^2, 2.5 min. (4) 9×10^{-8} A/cm^2, 11 min. (5) 8×10^{-7} A/cm^2, 15 min. (All cumulative).

to positive corona at a current of 6×10^{-7} Amp/cm^2 for 3.5 min results in a parallel shift of the C-V curves to the right. If all of the charge were located at the interface, a charge storage of approximately 4×10^{12} electrons/cm^2 is indicated. A similar test using an RCA oxide showed a charge storage of 8×10^{12} electrons/cm^2.

We then used negative corona on the BL sample with $J = 9 \times 10^{-8}$ A/cm^2. As shown by Curves 3 and 4 of Fig. 6.1, this produced a shift leftward, approaching (but never appreciably crossing over) the original curve. We conclude that the trapped electrons can be detrapped by the field of -4.8 MV/cm. The trapping of holes may also, at least in part, account for the observed leftward shift. If the corona current is raised to 4×10^{-7} A/cm^2, the C-V curve continues shifting to the left and a stretch-out is observed. A further experiment using a larger negative corona current (2.6×10^{-6} A/cm^2) and longer charging time produced a negative flatband voltage of 0.5 V which implies that positive charge is now stored in the oxide.

Figure 6.2 shows the result of a corona-charging experiment performed on the RCA sample of aluminum oxide. Upon exposure to negative corona at current of 4×10^{-7} A/cm^2 for 10 min, a $\sim$ 15 Volt negative flatband shift is noted and C-V stretch-out is seen. The bulk field in this case can reach 6 MV/cm and a large amount of positive charge is stored in the insulator. Following the exposure to negative corona, we applied positive corona to the sample. The C-V curve translates to the positive side as shown in Fig. 6.2 and stretch-out still exists.

(b) Samples with Thin ($\sim$ 200 Å) Al Gates

Figure 6.3 shows the results of an experiment using BL samples with thin ($\sim$ 200 Å) aluminum field plates. As shown by Curve 2, a bias of -20 volts for 5 minutes gives both positive flatband shift and stretch-out. If we then apply progressively larger values of positive voltage, the curves move to the right still further and the stretch-out disappears.

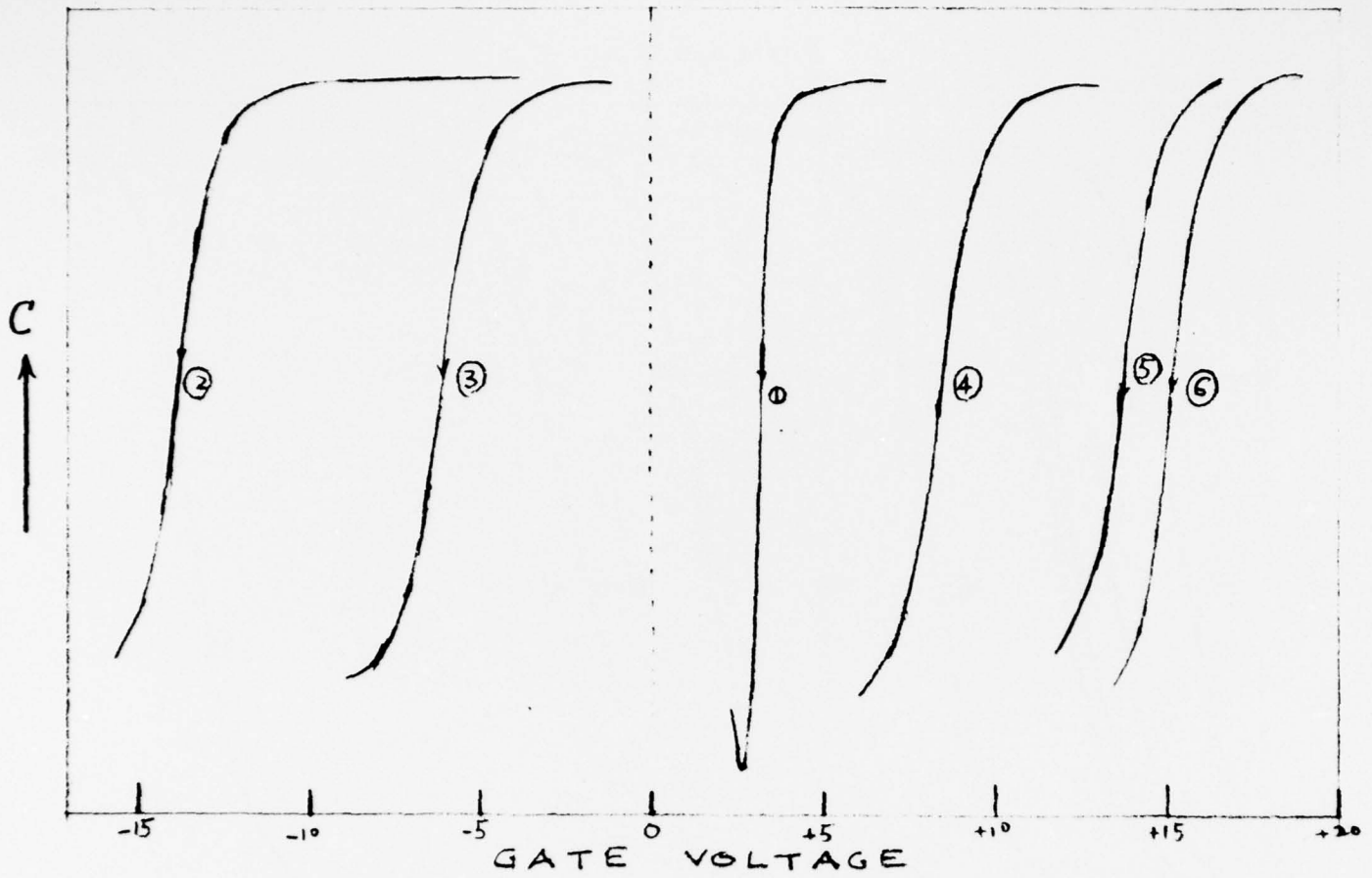


Fig. 6.2. Results of corona-charging experiment on RCA sample. (1) Fresh sample. (2) After negative corona, 4×10^{-7} A/cm^2, 10 min. After positive corona: (3) 1.6×10^{-7} A/cm^2, 1 min. (4) 1.6×10^{-7} A/cm^2, 2 min. (5) 1.6×10^{-7} A/cm^2, 3 min. (6) 1.6×10^{-7} A/cm^2, 5 min. (All cumulative).

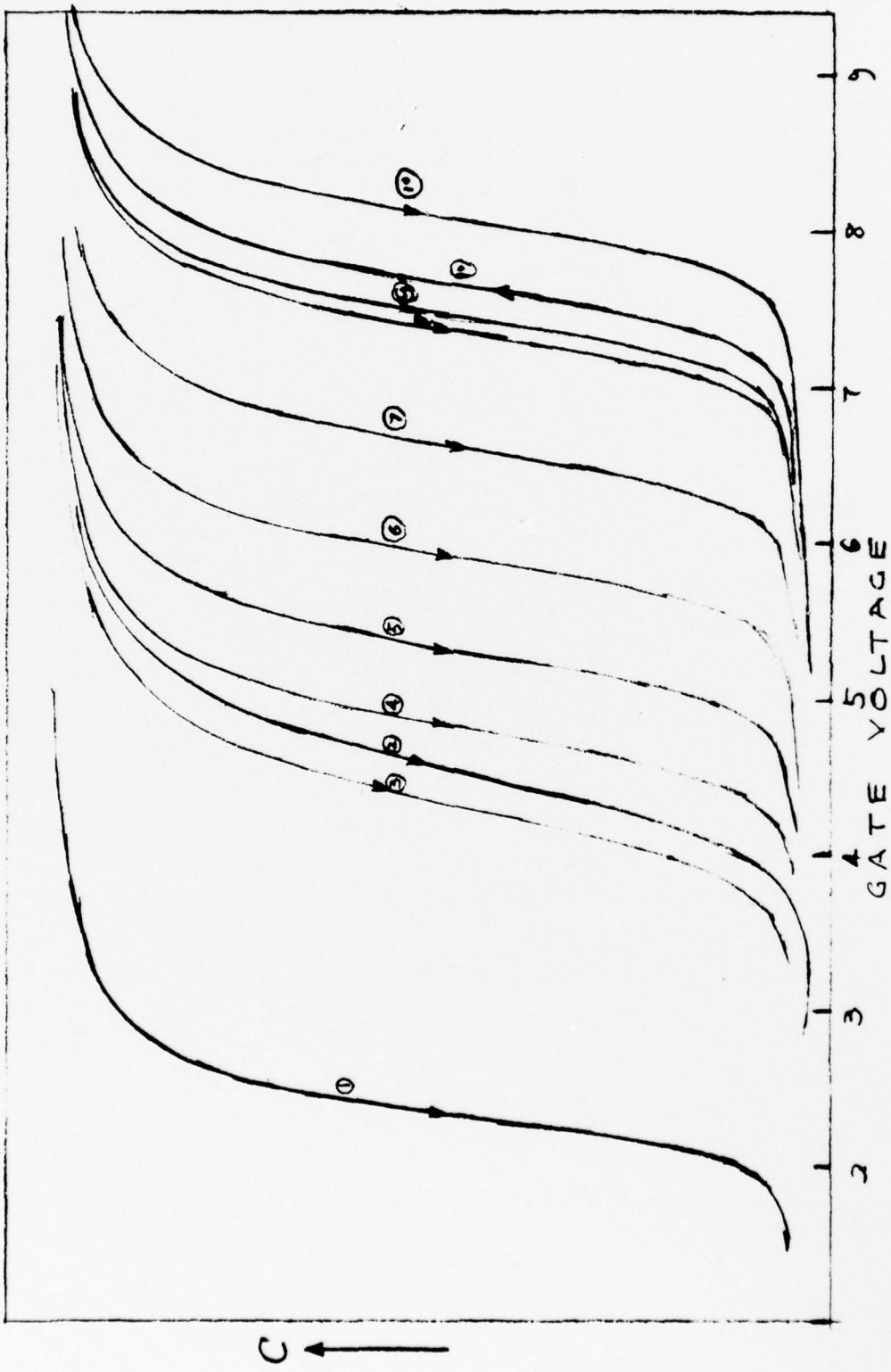


Fig. 6.3. Results obtained on BL MOS sample. (1) Fresh sample. Results of stressing, each for 5 min, cumulative: (2) -20 V. (3) 9 V. (4) 11 V. (5) 12 V. (6) 13 V. (7) 14 V. (8) 15 V. (9) 15 V. (10) 16 V.

6.3. Discussion

Positive bias causes field injection of electrons from the substrate into the aluminum oxide with subsequent electron trapping in the oxide. These trapped charges can be depopulated by a high negative field.

The negative flatband shift under negative corona indicates the storage of positive charges. The positive charges may originate from (a) holes tunneling from the substrate into Al_2O_3, or (b) electrons tunneling out of neutral centers, or (c) impact ionization.

The stretchout of the C-V curves may be due to the generation of interface states or to lateral nonuniformities in the trapped charge. For the RCA samples and the BL partially recovered samples, the injection of electrons causes a parallel translation to the right without stretchout. If the dispersion were due to a lateral nonuniformity, a reduction in dispersion might be expected because the electron injection would be enhanced in the region of more positive charge or less negative charge. It is suggested by this fact that the stretchout produced by negative bias is due to the generation of interface states. However, for the BL samples, since part of the stretchout can be removed by injecting electrons, we may suppose that nonuniform trapping exists in this sample.

After positive bias, the sample tends to go into deep depletion when the C-V curve is taken. This is because the holes in the inversion layer can tunnel into the Al_2O_3 and recombine with the trapped electrons near to the interface. This also produces a C-V hysterisis, as can be seen in Curve 10 of Fig. 6.3. After negative bias, no deep depletion is observed, because all the electrons near the interface have already tunneled back.

7. INTERFACE STATE GENERATION IN THE SCANNING ELECTRON MICROSCOPE

(P. Roitman collaborating)

7.1. Introduction

As part of our continuing study of metal-oxide-silicon (MOS) capacitors in the scanning electron microscope (SEM), we have investigated the electron-beam-induced formation of interface states at the silicon/oxide interface. We will discuss here the background motivating these experiments, the experimental technique used, and some preliminary results.

That penetrating, ionizing radiation causes damage in MOS devices has been appreciated for more than a decade.[58] Initially attention was focussed on positive charge, both holes and sodium ions, trapped at the interface. However, it was also appreciated that high energy radiation actually created new interface states.[59] For those interested in radiation-hard MOS transistors the trapped positive charge remains the major effect, for device and circuit characteristics are fatally altered by the charge long before interface states become a problem. As we will see below, typical radiation doses experienced in the SEM (and in electron beam lithography machines) can be much greater than the doses considered serious for radiation hardness. Under these conditions the beam-created interface states may become an appreciable factor. In particular, when attempting a semiquantitative model of the interaction between the SEM beam and defects in the silicon such as we have previously reported,[18] these interface states must be taken into account.

7.2. Experimental

All the samples used in this study were (100) Si wafers, chemically cleaned and thermally oxidized at 1000°C in steam to nominal thicknesses of 2000, 4000 and 6000 Å. Back contacts of either Al (for p-type) or doped Au (for n-type) were evaporated and diffused by heating in flowing N_2 to 450°C (Al) or 550°C (Au). Al gates were evaporated from a tungsten basket through a molybdenum mask, then sintered in flowing N_2 at 500° for 25 min. Individual capacitors were scribed, broken apart, and mounted in the SEM.

In the SEM, contact was made to the gate with a 5-mil tungsten wire etched to an $\sim$ 1μ diameter point. The sample was oriented in a previously described holder[25] so that it could be centered in the field of view without turning on the beam. Beam currents were measured before and after each exposure in a faraday cup consisting of a thin hollow tube with an aspect ratio greater than 100. During each exposure the beam was defocussed to form a spot $\sim$ 200μ in diameter. All these precautions were necessary to ensure lateral uniformity of exposure. A nonuniform exposure, which could be caused either by part of the gate being exposed longer than the rest or to nonuniform metallization, would produce results not easily distinguishable from surface states.

The samples were characterized using the high frequency (1 MHz) capacitance-voltage curves. From the measured accumulation and inversion capacitances the oxide thickness and silicon doping density were determined. The original flatband voltage was also identified.

The interface used to measure surface state density was that developed by Kuhn.[60] The essence of this technique is to measure the quasi-static capacitance and to compare the measured capacitance curve with one calculated for a device with no interface states. The quasi-static capacitance is measured by applying a slow ramp voltage to the device and observing the current which, for a constant value of dV/dt, is proportional to the capacitance. In our experiments the current was measured with a Kiethley 602 electrometer, the output of which was monitored by a Kiethley 106B digital voltmeter with BCD output. Typically 500 points were measured in a 25 volt sweep and stored in a minicomputer. A program in the computer produced plots of N_{ss} vs ψ. At higher radiation doses the low frequency C-V curve stretches out over more than 25 volts; in these cases the sweep rate was speeded up, which is permissible in the quasi-static approximation for large surface state densities.

The radiation exposure is expressed in terms of the energy deposited in the oxide. This quantity was calculated from the beam energy, beam current exposure time, oxide thickness and gate thickness by integrating

the loss curve as given by Everhart and Hoff.[61]

7.3. Results

We present here some preliminary results; a more complete report will be issued later.

Figure 7.1 shows typical high-frequency and quasi-static C-V curves before irradiation. The sample is p-type with $P_o = 1.25 \times 10^{15}$, $n_o = 1.68 \times 10^5$, $C_{FB} = 241$ pf, $L_{ox} = 2150$ Å, $V_{FB} = -5.0$ V. The high frequency and quasi-static curves do not exactly line up in accumulation; this is due to an imperfect back contact. The error introduced by such a mismatch, propagated as an error in the doping density, is not significant in determining the surface states, especially since the quasi-static oxide capacitance is not greatly affected by the back contact.

Figure 7.2 shows the surface state distribution corresponding to the quasi-static curve in Fig. 7.1 We have defined $\psi_s = 0$ at the Fermi level, which for this sample is 0.28 V above the valence band edge and 0.29 V below the intrinsic level.

Figure 7.3 shows two typical surface-state distributions after significant radiation doses. Note the change of scale. The gate was grounded during irradiation.

Figure 7.4 shows the rate of interface states generation vs dose for a sample which was irradiated to $\sim 10^6$ rad, then annealed for 1 hr. at 500°C in N_2, the re-irradiated. The value given for N_{ss} is the average value of N_{ss} in a range of $\pm$ .1 V around $\psi_s = 0$.

7.4. Discussion

Several comments are worth making, first about the experimental technique and then about the results.

Errors in Kuhn's technique arise in several ways. There is, of course, a basic error associated with the capacitance (current) measurement. In our case this includes linearity and offset errors in both the electrometer and the analog-to-digital conversion, linearity errors in the voltage ramp, and truncation errors caused by only storing three digits. We estimate these errors to be about $\pm$ 1-2 pf $\simeq \pm$ 0.5%. There

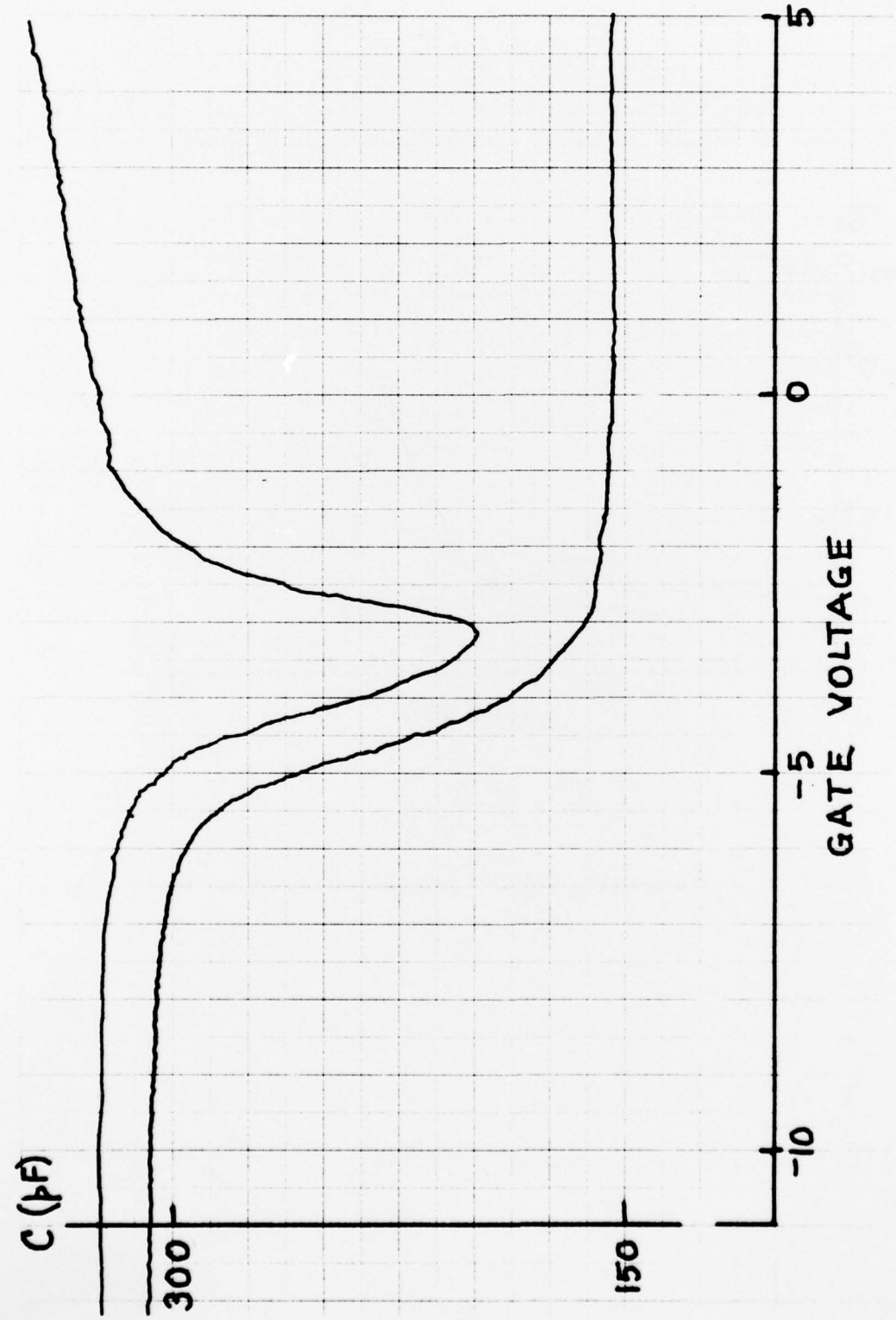


Fig. 7.1. High-frequency (1 MHz) and quasi-static C-V curves prior to irradiation. Sweep rate 0.1 V/sec.

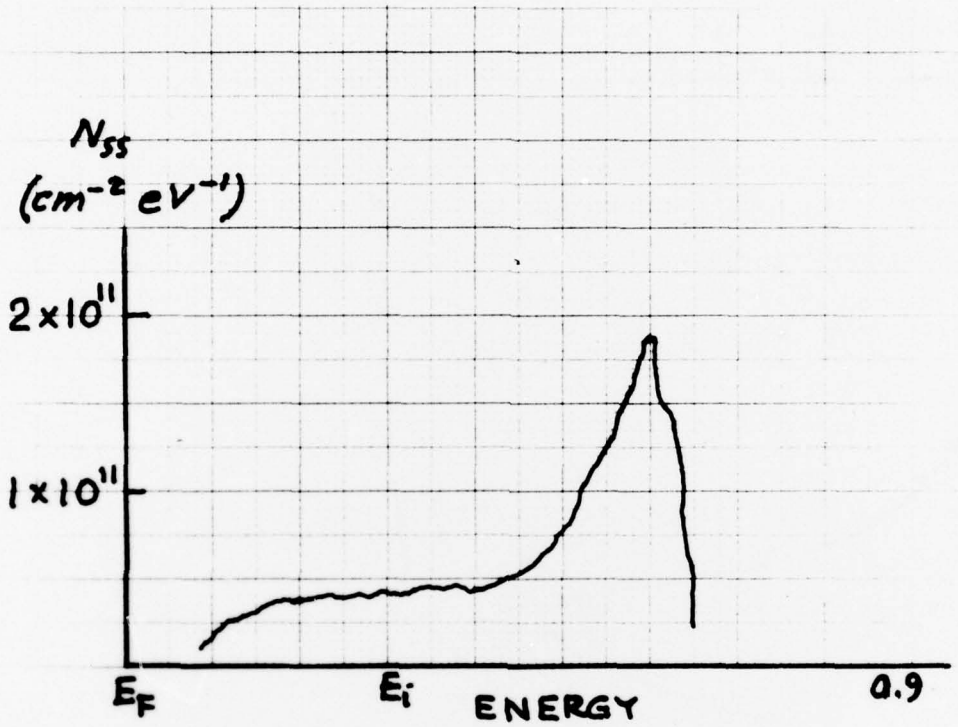


Fig. 7.2. Surface-state density calculated from curves of Fig.7.1.

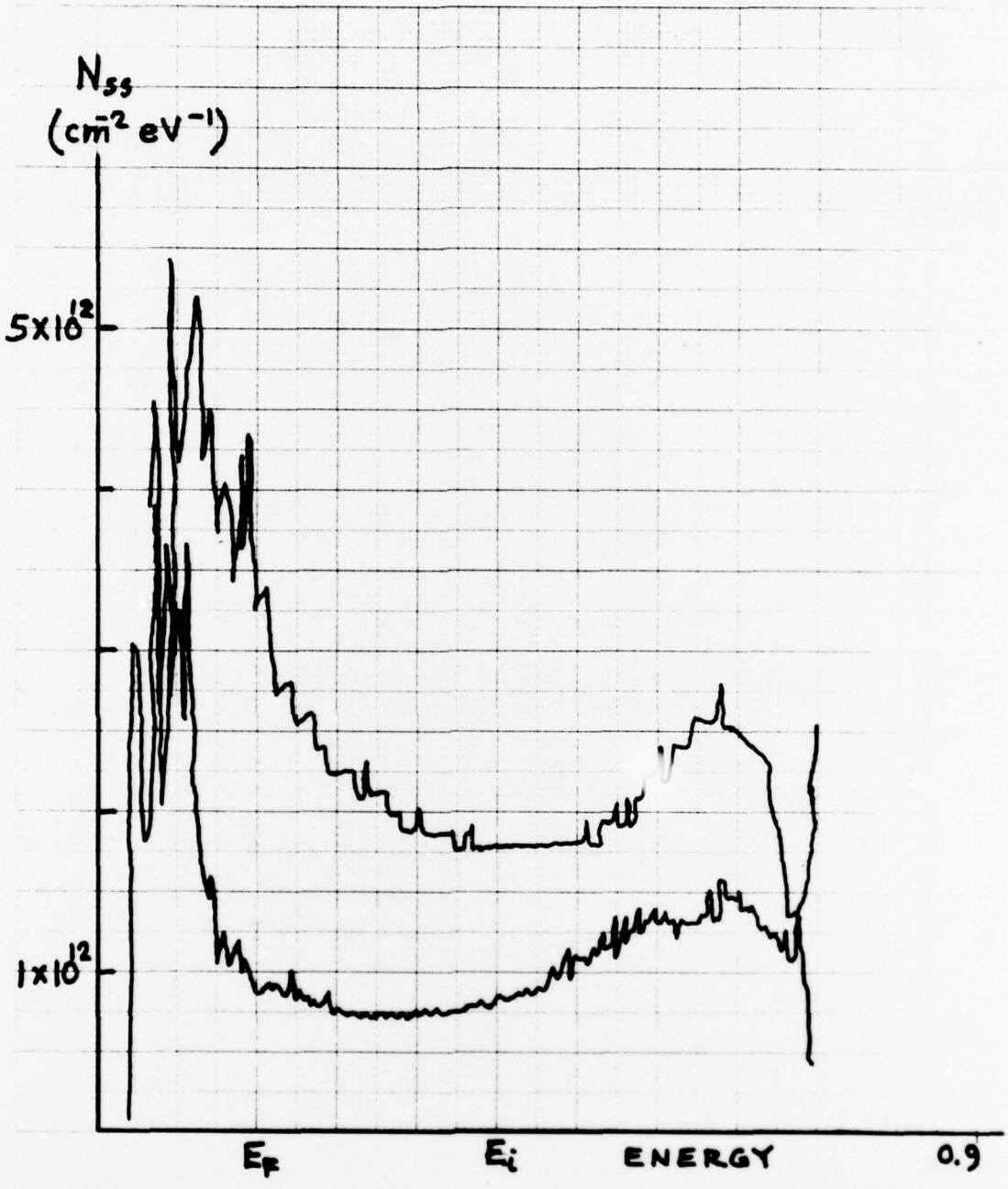


Fig. 7.3. Surface-state density after 25 KeV electron irradiation. Lower curve after dose of 4.2×10^5 rad (SiO_2). Upper curve after dose of 6.8×10^5 rad (SiO_2). Rad (SiO_2) is energy absorbed in the oxide; for these samples $\sim$ 1/25 of total energy.

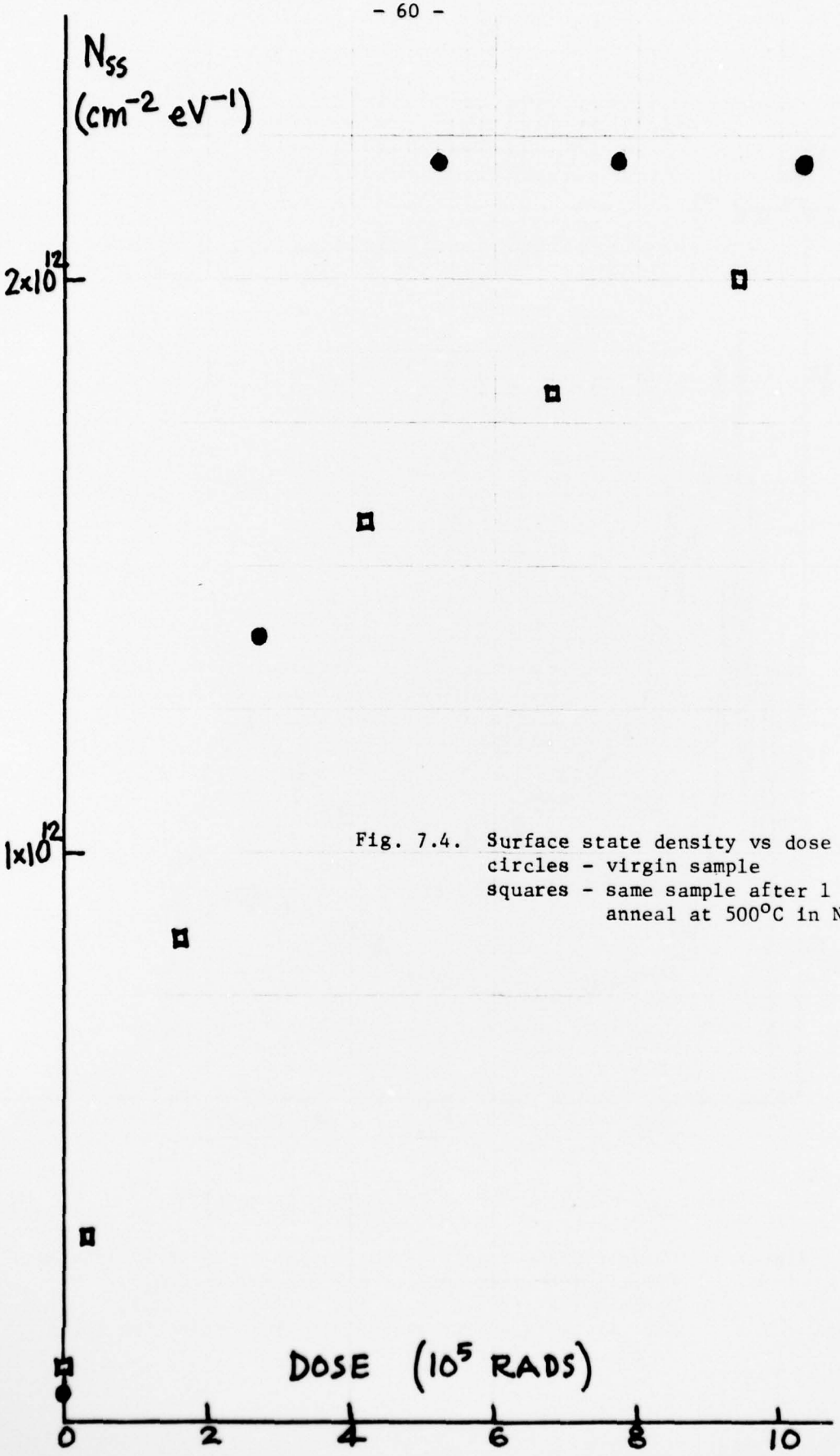


Fig. 7.4. Surface state density vs dose (SiO_2)
circles - virgin sample
squares - same sample after 1 hr. anneal at 500°C in N_2.

is also an error of $\lesssim$ 5% in the doping density caused by errors in the high-frequency curve due to imperfect back contacts. The high frequency C-V has been corrected empirically for line losses, but again there is a minimum error of $\pm$ 1 pf $\approx$ 0.5% here. Note that imperfect back contacts do not affect the displacement current measurement.

These errors affect the surface state curves in three ways. At midgap before irradiation the estimated error is a few times 10^{10}. In other words, the curve in Fig. 7.2 represents close to the minimum detectable density. We estimate this both from the numbers quoted above and from the reproducibility of these curves for adjacent capacitors on the same wafer and for the same capacitor before and after annealing. Near the band edges, the calculation involves a small difference between two terms of nearly the same magnitude, and calculational errors become large. The technique is certainly invalid closer than 0.2 eV to either band edge, and in practice the N_{ss} curve either oscillates wildly near the band edges or blows up positively or negatively. In this region the truncation error becomes important. At midgap after irradiation the error is also greater than 10^{10}, due to the extremely flattened nature of the C-V curve. Both absolute and quantization errors enter here and our feeling is that accuracy is approximately 10%. The "spikes" which appear in Fig. 7.3 are due to these errors.

Another type of error arises in the determination of an additive constant in computing surface potential. Especially for the heavily irradiated samples this additive constant is often difficult to determine accurately. Experience has indicated that the magnitude and shape of the N_{ss} curve are not particularly sensitive to errors in this constant and that although the position of the curve is more sensitive it is less so than one might expect. We assign an error of 0.05 eV to the position of the curve.

We conclude by noting that Kuhn's technique was chosen because it is relatively simple to use (given the minicomputer), is valid over most of the bandgap, and is reasonably sensitive in the range of interest. The conductance technique is, by contrast, more difficult to use, is not

valid over as wide a part of the bandgap, and in addition its sensitivity to lower values of surface state density was not of interest here.

The absolute magnitude of surface state density observed in Fig. 7.3 should not be taken too seriously, for several reasons. First, these were wet oxides not at all optimized for radiation hardness. In general it has been observed that radiation hardness is extremely process-dependent. As we have very imperfect control over our processing we cannot say anything else to this point. Second, in comparison with other studies oriented to radiation hardness, we are using relatively large doses. For the oxide shown in Figs. 7.3 and 7.4 the total dose absorbed by the whole device is about 25 times the dose we quote for the oxide alone. Nevertheless, these are relatively small doses in electron microscope terms: a dose of 2.5×10^5 rad represents a 10^{-10} amp. beam scanning the sample for 25 seconds. Third, and more fundamental, the experience of a large number of people who have studied clean surfaces and surfaces with small amounts of adsorbates over the last few years has been that changes in surface structure or surface adsorbates affect the density of states at the surface for many eV into the valence and conduction bands. We must assume that the same is true at the Si/SiO_2 interface, although the measurement of charges deep in the band appears to be currently impossible. The total charge in the density of states might be of real significance, but the charge in that small energy range represented by the bandgap is probably not. This is the basis for our choice of coordinates in Fig. 7.4. The middle 0.2 eV is where the measurement technique is most accurate, and we can assign no special significance to, for example, an integral of the surface state density over some fraction of the gap.

We interpret Fig. 7.4 to mean that a fairly prolonged anneal at $500^{\circ}C$ will, in fact, restore a device to approximately its original condition. Such a treatment is fairly drastic, however; in particular the back contact was seriously degraded. It is not completely clear at this point if the saturation observed at 2.2×10^{12} is real, since at that point the C-V curve was so flattened out that the technique may have been saturating.

REFERENCES

A. Publications, Reports, and Doctoral Dissertations Resulting From Work Done Under This Program.

1. M. A. Lampert, W. C. Johnson, and W. R. Bottoms, "Study of Electronic Transport and Breakdown in Thin Insulating Films," Semi-Annual Technical Report No. 1 (AFCRL-TR-73-0263), January 1973.

2. M. A. Lampert, W. C. Johnson, and W. R. Bottoms, "Study of Electronic Transport and Breakdown in Thin Insulating Films," Semi-Annual Technical Report No. 2 (AFCRL-TR-74-0076), July 1973.

3. N. M. Johnson, W. C. Johnson, and M. A. Lampert, "Electron Trapping in Ion-Implanted Silicon Dioxide Films on Silicon," Special Report No. 1 (AFCRL-TR-74-0133), January 1974. (This Special Report was based on N. M. Johnson's doctoral dissertation.)

4. W. C. Johnson, M. A. Lampert, and W. R. Bottoms, "Study of Electronic Transport and Breakdown in Thin Insulating Films," Semi-Annual Technical Report No. 3 (AFCRL-TR-74-0229), January 1974.

5. Z. A. Weinberg, W. C. Johnson, and M. A. Lampert, "Determination of the Sign of Carrier Transported Across SiO_2 Films on Silicon."
   (a) Appl. Phys. Lett. 25, 42 (1974).
   (b) Special Report No. 2 (AFCRL-TR-74-0206), April 1974.

6. D. Y. Yang, W. C. Johnson, and M. A. Lampert, "Scanning Electron Micrographs of Self-Quenched Breakdown Regions in Al-SiO_2-(100) Si Structures."
   (a) Appl. Phys. Lett. 25, 140 (1974).
   (b) Special Report No. 3 (AFCRL-TR-74-0278), June 1974.

7. W. C. Johnson and W. R. Bottoms, "Study of Electronic Transport and Breakdown in Thin Insulating Films," Semi-Annual Technical Report No. 4 (AFCRL-TR-74-0574), July 1974.

8. Z. A. Weinberg, "High-Field Transport in SiO_2 Films on Silicon Induced by Corona Charging," Ph.D. Dissertation, Princeton University, Sept. 1974.

9. D. Y. Yang, W. C. Johnson, and M. A. Lampert, "A Study of the Dielectric Breakdown of SiO_2 Films on Si by the Self-Quenching Technique," Special Report No. 4 (AFCRL-TR-74-0516), October 1974. (This Special Report was based on D. Y. Yang's doctoral dissertation.)

10. Z. A. Weinberg, D. L. Matthies, W. C. Johnson, and M. A. Lampert, "Measurement of the Steady-State Potential Difference Across a Thin Insulating Film in a Corona Discharge."
    (a) Special Report No. 5 (AFCRL-TR-74-0315), October 1974.
    (b) Rev. Sci. Instrum. 46, 201 (1975).

11. W. C. Johnson and W. R. Bottoms, "Study of Electronic Transport and Breakdown in Thin Insulating Films," Semi-Annual Technical Report No. 5 (AFCRL-TR-75-0157), January 1975.

12. Brian K. Ridley, "Mechanism of Electrical Breakdown in SiO_2 Films."
(a) J. Appl. Phys. 46, 998 (1975).
(b) Special Report No. 6 (AFCRL-TR-75-0182), March 1975.

13. W. R. Bottoms, D. Guterman, and P. Roitman, "Contrast Mechanisms in Electron Beam Images of Interface Structures."
(a) Special Report No. 7 (AFCRL-TR-75-0267), May 1975.
(b) J. Vac. Sci. Technol. 12, 134 (1975).

14. W. R. Bottoms and D. Guterman, "Electron Beam Probe Studies of Semiconductor-Insulator Interfaces."
(a) Special Report No. 8 (AFCRL-TR-75-0326), May 1975.
(b) J. Vac. Sci. Technol. 11, 965 (1974).

15. N. M. Johnson, W. C. Johnson, and M. A. Lampert, "Electron Trapping in Aluminum-Implanted Silicon Dioxide Films on Silicon," J. Appl. Phys. 46, 1216 (1975).

16. C. T. Shih, "A Study of the Effects of Low-Energy Electron Irradiation on MOS Capacitors," Ph.D. Dissertation, Princeton University, June 1975.

17. D. Y. Yang, W. C. Johnson, and M. A. Lampert, "A Study of the Dielectric Breakdown of Thermally Grown SiO_2 by the Self-Quenching Technique," 13th Annual Proceedings on Reliability Physics (IEEE), p. 10 (1975).

18. Daniel C. Guterman, "Electron-Beam Induced Imaging and Analysis of Internal Structure in the Metal-Insulator-Semiconductor Structure," Ph.D. Dissertation, Princeton University, November 1975.

19. Walter C. Johnson, "Mechanisms of Charge Buildup in MOS Insulators," IEEE Trans. Nucl. Science NS-22, 2144 (Dec. 1975).

20. Z. A. Weinberg, W. C. Johnson, and M. A. Lampert, "High-Field Transport in SiO_2 on Silicon Induced by Corona Charging of the Unmetallized Surface," J. Appl. Phys. 47, 248 (1976).

21. C. C. Chang, "Study of Lateral Nonuniformities and Interface States in MIS Structures," Ph.D. Dissertation, Department of Electrical Engineering, Princeton University, February 1976.

22. H. S. Lee, "High-Field Effects in SiO_2 Films on Silicon," Ph.D. Dissertation, Department of Electrical Engineering, Princeton University, February 1976.

23. Walter C. Johnson, "Study of Electronic Transport and Breakdown in Thin Insulating Films," Final Report, Contract F19628-72-C-0298 (RADC-TR-76-158), May 1976.

24. S. Baidyaroy, M. A. Lampert, B. Zee, and R. U. Martinelli, "Monte Carlo Studies of Hot-Electron Distributions in Thin Insulating Films: I. Constant Mean Free Path and a One-Dimensional Simulation," J. Appl. Phys. 47, 2103 (1976).

25. Walter C. Johnson, "Study of Electronic Transport and Breakdown in Thin Insulating Films," Semi-Annual Technical Report No. 1, Contract DAAG53-76-C-0059 (NVL-0059-001),1 June 1976.

26. S. Baidyaroy, M. A. Lampert, B. Zee, and R. U. Martinelli, "Monte Carlo Studies of Hot-Electron Distributions in Thin Insulating Films: II. Energy-Dependent Mean Free Path and Instability," Special Technical Report No. 1, Contract DAAG53-76-C-0059 (NVL-0059-002), 15 November 1976.

B. OTHER REFERENCES

27. R. Williams, Phys. Rev. 140, A569 (1965).

28. D. M. Boulin, private communication.

29. R. J. Powell, J. Appl. Phys. 40, 5093 (1969).

30. M. H. Woods and R. Williams, J. Appl. Phys. 47, 1082 (1976).

31. R. J. Powell and G. F. Derbenwick, IEEE Trans. Nucl. Sci. NS-18, 99 (Dec. 1971).

32. R. J. Powell and G. W. Hughes, Annual Report, 31 Jan. 1975, Office of Naval Research, Contract N0014-74-C-0185.

33. E. H. Nicollian, A. Goetzberger, and C. N. Berglund, Appl. Phys. Lett. 15, 174 (1969).

34. J. F. Verwey, Appl. Phys. Lett. 21, 417 (1972).

35. J. F. Verwey, J. Appl. Phys. 43, 2273 (1972).

36. E. H. Snow, A. S. Grove, and D. J. Fitzgerald, Proc. IEEE 55, 1165 (1967).

37. T. H. Ning, J. Appl. Phys. 47, 3203 (1976).

38. R. J. Powell, IEEE Trans. Nucl. Sci. NS-22, 2240 (1975).

39. E. Harari, S. Wang, and B. S. H. Royce, J. Appl. Phys. 46, 1310 (1975).

40. H. E. Boesch, Jr., F. B. McLean, J. M. McGarrity and G. A. Ausman, Jr., IEEE Trans. Nucl. Sci. NS-22, 2163 (1975).

41. F. B. McLean, H. E. Boesch, Jr., and J. M. McGarrity, to be published in IEEE Trans. Nucl. Sci., Dec. 1976.

42. H. H. Sander and B. L. Gregory, IEEE Trans. Nucl. Sci., NS-22, 2157 (Dec. 1975).

43. J. R. Srour, S. Othmer, O. L. Curtis, Jr., and K. Y. Chiu, to be published.

44. O. L. Curtis, Jr., J. R. Srour, and K. Y. Chiu, J. Appl. Phys. 45, 4506 (1974).

45. R. C. Hughes, Appl. Phys. Lett., 26, 436 (1975).

46. R. J. Powell, J. Appl. Phys., 46, 4557 (1975).

47. K. H. Zaininger, Appl. Phys. Lett., 8, 140 (1966).

48. R. C. Hughes, Phys. Rev. Lett., 35, 449 (1975).

49. R. C. Hughes, Phys. Rev. Lett., 30, 1333 (1973).

50. E. H. Nicollian, C. N. Berglund, P. F. Schmidt and J. M. Andrews, J. Appl. Phys., 42, 5654 (1971).

51. J. H. Thomas III, J. Appl. Phys. 44, 811 (1973).

52. J. H. Thomas III and F. J. Feigl, J. Phys. Chem. Solids, 33, 2197 (1972).

53. R. Williams, Phys. Rev. 140, A569 (1965).

54. T. H. Ning, J. Appl. Phys. 47, 3203 (1976).

55. T. H. Ning, C. M. Osburn, and H. N. Yu, Appl. Phys. Lett. 26, 248 (1975).

56. R. J. Powell and G. W. Hughes, IEEE Transactions on Nuclear Science NS-21, 179 (Dec. 1974).

57. R. H. Walden, J. Appl. Phys. 43, 1178 (1972).

58. (a) H. L. Hughes and R. A. Giroux, Electronics 37, 58 (1964).
(b) K. H. Zaininger and A. G. Holmes-Siedle, RCA Rev. 28, 208 (1967).

59. (a) L. L. Sivo, H. L. Hughes, and E. E. King, IEEE Trans. Nucl. Sci. NS-19, 313 (1972).
(b) T. P. Ma, G. Scoggan and R. Leone, Appl. Phys. Lett. 27, 2, 61 (1975).
(c) T. P. Ma, Appl. Phys. Lett. 27, 11, 615 (1975).

60. M. Kuhn, Sol. St. El. 13, 873 (1970).

61. T. E. Everhart and P. H. Hoff, J. Appl. Phys. 42, 13, 5837 (1971).